ANL/ESD-14/2

Geothermal Power Production: Alternative Scenarios and Critical Issues

Energy Systems Division

About Argonne National Laboratory
Argonne is a U.S. Department of Energy laboratory managed by UChicago Argonne, LLC under contract DE-AC02-06CH11357. The Laboratory's main facility is outside Chicago, at 9700 South Cass Avenue, Argonne, Illinois 60439. For information about Argonne and its pioneering science and technology programs, see www.anl.gov.

DOCUMENT AVAILABILITY

Online Access: U.S. Department of Energy (DOE) reports produced after 1991 and a growing number of pre-1991 documents are available free via DOE's SciTech Connect (http://www.osti.gov/scitech/)

Reports not in digital format may be purchased by the public from the National Technical Information Service (NTIS):
U.S. Department of Commerce
National Technical Information Service
5301 Shawnee Rd
Alexandra, VA 22312
www.ntis.gov
Phone: (800) 553-NTIS (6847) or (703) 605-6000
Fax: (703) 605-6900
Email: **orders@ntis.gov**

Reports not in digital format are available to DOE and DOE contractors from the Office of Scientific and Technical Information (OSTI):
U.S. Department of Energy
Office of Scientific and Technical Information
P.O. Box 62
Oak Ridge, TN 37831-0062
www.osti.gov
Phone: (865) 576-8401
Fax: (865) 576-5728
Email: **reports@osti.gov**

Disclaimer
This report was prepared as an account of work sponsored by an agency of the United States Government. Neither the United States Government nor any agency thereof, nor UChicago Argonne, LLC, nor any of their employees or officers, makes any warranty, express or implied, or assumes any legal liability or responsibility for the accuracy, completeness, or usefulness of any information, apparatus, product, or process disclosed, or represents that its use would not infringe privately owned rights. Reference herein to any specific commercial product, process, or service by trade name, trademark, manufacturer, or otherwise, does not necessarily constitute or imply its endorsement, recommendation, or favoring by the United States Government or any agency thereof. The views and opinions of document authors expressed herein do not necessarily state or reflect those of the United States Government or any agency thereof, Argonne National Laboratory, or UChicago Argonne, LLC.

ANL/ESD-14/2

Geothermal Power Production: Alternative Scenarios and Critical Issues

by
J.L. Sullivan, T. Stephens, and M. Wang
Energy Systems Division, Argonne National Laboratory

February 2014

CONTENTS

ACKNOWLEDGMENTS vii
NOTATION ix
ABSTRACT 1
1 INTRODUCTION 3
2 METHOD 7
3 ASSESSMENT OF THE OPERATIONS AND MAINTENANCE STAGE AND DECOMMISSIONING STAGE OF THE LIFE CYCLE ANALYSIS 9
3.1 Previous Estimates of O&M and Decommissioning Values for Fossil Energy Consumption and GHG Emissions 9
3.2 O&M LCA Estimates for Power Generating Technologies 11
3.2.1 O&M for Renewable Power Generating Technologies 11
3.2.2 O&M for Fossil Power Generating Technologies 13
3.3 Key Findings about Power Plant O&M Burdens 14
4 ALTERNATIVE SCENARIOS FOR GEOTHERMAL POWER PRODUCTION 15
4.1 New EGS, HT-F, and HT-B Scenarios 16
4.2 Results for New Geothermal System Scenarios 16
4.3 Results on a Capacity Basis 20
4.4 Key Findings from the Analysis Alternative Geothermal Plant Scenarios 21
5 GEOTHERMAL EXPLORATION 23
5.1 Methods for Geothermal Well Field Exploration 23
5.2 Geothermal Well Field Exploration Studies 24
5.3 Exploration Model for Geothermal Life Cycle Assessments 26
5.3.1 Well Assumptions 27
5.4 Exploration Results 28
5.5 Key Findings on Well Field Exploration Model Results 33
6 GHG EMISSIONS FROM CALIFORNIA GEOTHERMAL POWER PRODUCTION 35
6.1 Geothermal GHG Emissions Background 35
6.2 Geothermal Plant Locations 36
6.3 GHG Emissions and Electricity from California Geothermal Power Plants 37
6.4 Results: California GHG Emissions 38
6.5 Key Findings on Geothermal GHG Emissions 41
7 GEOTHERMAL VERSUS OTHER POWER GENERATING TECHNOLOGIES 43

CONTENTS (CONT.)

8 CONCLUSIONS....47
9 REFERENCES....49
APPENDIX A: Supporting Material....53

FIGURES

1 System Boundary for GREET Electricity Modules....8
2 Infrastructure Energy Ratio Values on a Percentage Basis....12
3 Infrastructure GHG Emission Rates on a Percentage Basis....12
4 Hydrothermal Plant Cycle GHG Emissions Versus Total Length of Wells per Megawatt of Capacity for Binary and Flash Scenarios....18
5 EGS Plant Cycle GHG Emissions Versus Total Length of Wells per Megawatt of Capacity for Binary and Flash Scenarios....18
6 Plant Cycle GHG Emissions Versus Plant Capacity for the Geothermal Power Production Scenarios Listed in Legend....20
7 Dependencies of the Number of Exploration Wells Needed to Develop a Geothermal Plant on Plant Capacity and Resource Depth....25
8 Well Field Drilling Cost and Number of Production Wells Versus Plant Capacity for Plants in Nevada....26
9 Cement MPRs for Various Geothermal Technologies....29
10 Amounts of Cement Needed to Build Power Plants and Well Fields....31
11 Plant Cycle Fossil Energy Ratios for Several Geothermal Energy Technologies....32
12 Plant Cycle GHG Emission Ratios for Several Geothermal Energy Technologies....32
13 Comparison of 2008–2012 GHG Emission Rates from California HT-F Plants, Both Flash and Dry Steam....39
14 GHG Emission Rate Cumulative Distribution Functions for Global and 2012 California HT-F Capacities....40
15 Components of Life Cycle GHG Emissions at the Plant Gate for a Range of Power Generating Technologies....43
16 Components of the Life Cycle Energy Ratio at the Plant Gate for a Range of Power Generating Technologies....44
A-1 EGS Binary and Flash Scenario LCOE and Plant Cycle GHG Emissions: Reference Cases Versus Improved Cases....56

FIGURES (CONT.)

A-2 Hydrothermal Binary and Flash Plant LCOE and Plant Cycle GHG Emissions: Reference Cases Versus Improved Cases 57

A-3 Steel Material-to-Power Ratios for the Indicated Geothermal Technologies 57

A-4 Diesel Material-to-Power Ratios for the Indicated Geothermal Technologies 58

A-5 Water Material-to-Power Ratios for the Indicated Geothermal Technologies....58

A-6 Cement Material-to-Power Ratios for the Indicated Geothermal Technologies....59

TABLES

1 Energy and GHG Ratios from White and Kulcinski for Plant Cycle, O&M, and Decommissioning Stages 9

2 Comparison of Fossil Energy and GHG Ratios Estimated by Argonne with Results from the Literature....14

3 Details on Geothermal Scenarios Previously Analyzed....15

4 Average Geothermal GHG Emission Rates in Various Years in California....39

A-1 Modeling Details and Corresponding Energy and GHG Ratio Values for a Series of Power Production Technologies by Life Cycle Stage....53

A-2 GETEM Input for Alternative Enhanced Geothermal System Plant Scenario Pairs: Reference Cases and Improved Cases....54

A-3 GETEM Input for Alternative Hydrothermal Plant Scenario Pairs: Reference Cases and Improved Cases....55

A-4 GHG Emission and Energy Ratios for the New Geothermal Power Plant Scenarios Given in Tables A-2 and A-3: Reference Cases and Improved Cases 56

A-5 Material-to-Power Ratios for Well Field Characterization 60

A-6 2008 GHG Emissions, Electricity Generation, and Emission Rates for California Geothermal Power Production 61

A-7 2009 GHG Emissions, Electricity Generation, and Emission Rates for California Geothermal Power Production 61

A-8 2010 GHG Emissions, Electricity Generation, and Emission Rates for California Geothermal Power Production 62

A-9 2011 GHG Emissions, Electricity Generation, and Emission Rates for California Geothermal Power Production 62

TABLES (CONT.)

A-10 2012 GHG Emissions, Electricity Generation, and Emission Rates for California Geothermal Power Production 63

A-11 Averages of and Ranges for Fuel Use Cycle GHG Emissions from California HT-F Plants for the Years 2008, 2009, and 2010.....63

ACKNOWLEDGMENTS

The Geothermal Technologies Office in the U.S. Department of Energy's Office of Energy Efficiency and Renewable Energy sponsored this work. Argonne National Laboratory is a DOE laboratory managed by UChicago Argonne, LLC, under Contract No. DE-AC02-06CH11357. We are grateful to Arlene Anderson of the DOE Geothermal Technologies Program for her guidance and input. We also wish to acknowledge Kyle Snyder (Ormat) and Lisa Shevenell (ATLAS Geosciences Inc. and Nevada Bureau of Mines and Geology at the University of Nevada, Reno) for their very helpful comments on well field exploration. And we want to thank Greg Mines of Idaho National Laboratory for his contributions in many very helpful discussions.

This page intentionally blank.

NOTATION

ACRONYMS AND ABBREVIATIONS

Bio-UB	biomass-fired utility boiler
BWR	boiling water reactor (nuclear)
C	capacity (MW)
CARB	California Air Resources Board
CAP	criteria air pollutant
CDF	cumulative distribution function
CEC	California Energy Commission
CEPA	California Environmental Protection Agency
cf	capacity factor
CSP	concentrated solar power
dcm	decommissioning (a life cycle stage)
E_{out}	electricity out (total plant lifetime electricity delivered)
E_{pc}	energy used in plant cycle
EIA	Energy Information Administration
EGS	enhanced geothermal system
EGS-B	enhanced geothermal system – binary
EGS-F	enhanced geothermal system – flash
EIO	economic input output
$\mathcal{E}_j$	fossil energy ratio: fossil energies (kWh) consumed in life cycle stage "j" per kWh of plant lifetime electricity output
$\mathcal{E}_{pc}$	$\mathcal{E}_j$ for the plant cycle (pc) stage
$\mathcal{E}_{tot}$	$\mathcal{E}_j$ for the entire (tot) life cycle across all stages
fc	fuel cycle (a life cycle stage, includes fu and fp)
FGD	flue gas desulfurization
fp	fuel production (a life cycle stage)
fu	fuel use (a life cycle stage)
GEA	Geothermal Energy Association
GETEM	Geothermal Electricity Technology Evaluation Model
gf	greenfield
GHG	greenhouse gas(es)
ghg_j	greenhouse gas ratio: GHGs (grams) emitted in life cycle stage "j" per kWh of plant lifetime electricity output
ghg_{pc}	ghg_j for the plant cycle (pc) stage
ghg_{tot}	ghg_j for the total (tot) life cycle
GIS	geographic information system
GPGE	geopressured gas and electricity (describes power plant with two outputs)

$GPGE_{gf}$	GPGE from greenfield sites
$GPGE_{rw}$	GPGE from reworked sites
GREET	Greenhouse Gases, Regulated Emissions, and Energy in Transportation Model
HT-B	hydrothermal binary power plant technology
HT-F	hydrothermal flash and dry steam power plant technology
I	injection (well)
IGCC	integrated gasification combined cycle
InSAR	interferomeric synthetic aperture radarISO International Standards Organization
LCA	life cycle analysis
LCI	life cycle inventory analysis
LCOE	levelized cost of electricity (¢/kWh)
LEBS	low-emission boiler system (coal-fired power plant)
LHV	low heat value
LiDAR	term created by combining "light" and "radar"
LT	lifetime of plant
M_{st}	materials for well field stimulation (diesel and water only)
MPR	material-to-power ratio
MPW	material per wellMW_{el} output capacity of an electricity power plant
MW_{mx}	output capacity of plants with more than one output
MW_{th}	output capacity of plant that produces combustion products (e.g., natural gas)
mx	plants with mixed outputs (e.g., electricity and natural gas)
N	nuclear
N_{fc}	number of failed confirmation wells
N_I	number of injection wells
N_P	number of production wells
NGCC	natural gas combined cycle
NSPS	New Source Performance Standards (coal-fired power plant)
o&m	operations and maintenance (a life cycle stage)
O&M	operations and maintenance (a life cycle stage)
P	production (well)
pc	plant cycle (a life cycle stage, entails on-site plant construction activities and the production of the materials that make up structures and equipment)
PCA	process chain analysis
$PM_{2.5}$	particulate matter with a mean aerodynamic diameter of 2.5 μm or less
PM_{10}	particulate matter with a mean aerodynamic diameter of 10 μm or less
PV	photovoltaic
PWR	pressurized water reactor (nuclear)

rw	reworked
SC	subcritical (coal combustion)
SCR	selective catalytic reduction
TGH	thermal gradient hole
th	thermal
tot	total of all life cycle stages
VOC	volatile organic compound
3YA	three-year averaged

CHEMICALS

CH_4	methane
CO	carbon monoxide
CO_2	carbon dioxide
H_2O	water
H_2S	hydrogen sulfide
NO_x	nitrogen oxides
N_2O	nitrous oxide
SO_x	sulfur oxides

UNITS OF MEASURE

Btu	British thermal unit
°C	degree(s) Celsius
d	day(s)
g	gram(s)
gal	gallon(s)
hp	horsepower
kg	kilogram(s)
kWh	kilowatt-hour(s)
L	liter(s)
m	meter(s)
m^3	cubic meter(s)
MJ	megajoule(s)
mt	metric ton(s) or tonne(s)
MW	megawatt(s)
s	second(s)
tonne(s)	metric ton(s) or mt
yr	year(s)
µm	micrometer(s)

This page intentionally blank.

GEOTHERMAL POWER PRODUCTION: ALTERNATIVE SCENARIOS AND CRITICAL ISSUES

by

J.L. Sullivan, T. Stephens, and M. Wang

ABSTRACT

This is the last in a series of reports that completes the life cycle analyses (LCAs) of geothermal power production technologies conducted by Argonne National Laboratory. It addresses the remaining critical issues pertaining to the LCAs of geothermal electricity production: the relative contributions from plant operations and maintenance (O&M), from decommissioning (dcm), from well field exploration, and from plant operational greenhouse gas (GHG) emissions to the total life cycle performance of geothermal power plants. Contributions from O&M and dcm to the performance of other power generating technologies are also discussed. Also included in this study are LCA results for a new series of scenarios for geothermal power production. Our analysis uses fossil fuel energy consumption and GHG emissions per unit of lifetime electricity output (referred to as the fossil energy and GHG ratios, respectively) as the life cycle metrics for quantifying life cycle stage contributions to their corresponding totals, which were subsequently used for comparing the environmental performance of geothermal and other electric power production plants. Based on literature results, we concluded that the contribution from dcm to both ratios is negligible for power plants in general. Further, we found that the contribution from O&M to both ratios is generally significant for facilities with no fuel cycle (fuel production and use) burdens. In the case of geothermal power production, O&M contributes about 20% to the total for enhanced geothermal power plants, 10% for geothermal binary plants, and about 25% of the energy ratio for geothermal flash and dry steam plants. However, due to operational GHG emissions that are unique among geothermal power plants, O&M contributes only about 1% of total GHG ratios for flash and dry steam plants. These GHG emissions arise when the geofluids of these plants become exposed to the atmosphere, thus releasing dissolved GHGs. The amount of GHG emissions from these plants had a wide range. However, we found that 85% of California's running capacity in flash and dry steam plants released 160 grams or less per kilowatt-hour of electricity produced.

We developed an exploration model to account for core hole, slim hole, and confirmation well drilling that includes a probability of success for confirmation well drilling. The model shows that well field exploration represents about 20% of the total life cycle burden for large geothermal plants with numerous wells and 32% of the burden for small plants with few wells.

We also analyzed a set of geothermal scenario pairs. The objective was to identify geothermal scenarios with a lower levelized cost of electricity and lower life cycle burdens. A comparison of reference with improved cases within each pair revealed that the improved cases demonstrated a lower levelized cost of electricity and lower fossil energy consumption and GHG metrics. The scenario pairs covered a range of plant capacities, well numbers and depths, resource temperatures, and plant lifetimes. Finally, we found that compared to fossil-fuel generation of electricity, both flash and dry steam geothermal electricity generation result in fewer GHG emissions: on average, only one-fifth of the GHG emissions per kilowatt-hour from a natural gas combined-cycle plant, and one-tenth of those from a coal-fired plant. Moreover, these fractions were much smaller when the fossil plants were compared with plants that use geothermal binary technology.

1 INTRODUCTION

Forty percent of primary energy consumption in the United States is devoted to generating electric power, and most of that energy is derived from fossil resources (EIA 2010a). Concerns about climate change and energy security have prompted a reevaluation of our fossil fuel consumption. Toward that end, some states have already adopted "Renewable Portfolio Standards" and are thus adding more wind, solar, and other types of renewable energy to their sets of generating technologies. The Energy Information Administration (EIA) projects that renewable electricity, which accounted for about 10.4% of U.S. electricity generation in 2010, will increase to about 15.2% by 2035 (EIA 2010a). It projects that most of the increase will come from additional wind turbines and biomass combustion plants. Geothermal electricity generation, another renewable generating technology whose use could significantly reduce fossil fuel consumption, is expected to grow from 3.7% to 6.1% of renewable power over that same time frame (EIA 2010a). It could perhaps grow to a significantly larger percentage if widespread deployment of enhanced geothermal systems (EGSs) is realized. This technology is anticipated to operate on the more broadly available, lower-temperature geofluids.

In previous reports in this series, we presented life-cycle assessment (LCA) metrics (Sullivan et al. 2010, 2011, 2012, 2013; Clark et al. 2010, 2011) for geothermal power technologies and compared them to metrics for "other" power technologies for electricity production. The LCA metrics serve as measures of environmental performance per unit of service provided — in this case one kilowatt-hour (1 kWh) of electricity. The "other" category included coal-fired technologies (boiler and integrated gasification combined cycle [IGCC]); natural-gas-fired technologies (natural gas combined cycle [NGCC]); and nuclear technologies (pressurized water reactors [PWRs] and boiling water reactors [BWRs]). Representing renewable technologies were hydroelectric, photovoltaic (PV), wind, biomass combustion boiler, biomass IGCC, and concentrated solar power (CSP). The geothermal technologies covered in those studies were hydrothermal flash and dry steam (HT-F), hydrothermal binary (HT-B), EGS, and two variants of geopressured gas and electricity (GPGE), one from reworked sites (GPGE-rw) and the other from greenfield sites (GPGE-gf). All of our previous geothermal studies addressed only EGS binary (EGS-B); in this report results from EGS flash (EGS-F) are introduced.

To generate our life cycle results for the other power production technologies, we conducted surveys of the literature for data. For data on geothermal technologies, we developed computer models to estimate the material content of power plants, well fields, and aboveground piping that connect wells with plants. From these material estimates, two plant cycle (pc) metrics (this cycle entails on-site plant construction activities and the production of the materials that make up structures and equipment) were computed: the amount of fossil energy consumed and the amount of greenhouse gases (GHGs) emitted per kilowatt-hour of electricity produced — $\mathcal{E}_{pc}$ and ghg_{pc}, respectively.

In our previous work [cited above], we added fuel cycle (fc) burdens to our plant cycle energy and emission ratios, yielding estimates of the total life cycle ratios $\mathcal{E}_{tot}$ and ghg_{tot}. The fc includes both fuel production (fp) and fuel use (fu); for example, it includes the mining and transportation of coal and its subsequent combustion to produce electricity. For environmental

performance assessments, we compared $\mathcal{E}_{tot}$ and ghg_{tot} for the various geothermal and other power production technologies. Some of the key conclusions that we drew from our previous work (Sullivan et al. 2010, 2011, 2012, 2013) follow here:

- Fossil plants have by far the greatest $\mathcal{E}_{tot}$ and ghg_{tot} values for all the technologies.
- Of the renewable technologies, biomass combustion, HT-F, and GPGE have the highest ghg_{tot} due to operational GHG emissions.
- Due to their lower material requirements per megawatt (MW) of capacity, thermoelectric plants (coal, natural gas, nuclear, and biomass combustion) have much lower $\mathcal{E}_{pc}$ and ghg_{pc} values than do PV, wind, hydroelectric, CSP, and geothermal plants.
- $\mathcal{E}_{pc}$ and ghg_{pc} values for geothermal plants vary widely depending on the well depth and type of system condenser (air versus water) used.
- Except for PV technology, cement/concrete and steel are the materials that are used to the greatest extent by far across all the electricity generation technologies.

Most of these results have been incorporated into Argonne's Greenhouse Gases, Regulated Emissions and Energy in Transportation (GREET) model (GREET1 2012).

Our most recent report (Sullivan et al. 2012) has preliminary results on the impact of well field exploration on the environmental footprint from geothermal power production. That report also includes a preliminary analysis of GHG emissions incurred during geothermal plant operations. In addition, the report analyzes the use of supercritical (SC) carbon dioxide (CO_2) as a substitute for brine geofluids in EGSs, especially when available water resources are not adequate for conventional EGS. The system was analyzed as a coupled EGS and coal plant, in which the latter provides the SC CO_2. Depending on the CO_2 capture rate, the coupled system showed a large reduction in GHG emissions relative to those from a corresponding coal plant operating on its own. Finally, the report (Sullivan et al. 2012) also assesses criteria air pollutant (CAP) emission rates (in grams per kWh [g/kWh]) from geothermal and other power plants. The former were added to GREET1 (2012), along with newly updated values for fossil-based power production. The CAP emissions include methane (CH_4), nitrous oxide (N_2O), other nitrogen oxides (NO_x), carbon monoxide (CO), volatile organic compounds (VOCs), sulfur oxides (SO_x), particulate matter with a diameter of 10 micrometers (μm) or less (PM_{10}), and particulate matter with a diameter of 2.5 μm or less ($PM_{2.5}$). GREET1 (2012) now includes electrical power generation from fossil fuels, nuclear fuels, and renewable energy sources, including solar, hydro, wind, and geothermal power production with hydrothermal and water-EGS technologies.

This report presents results on the remaining tasks needed to conclude our LCA studies of geothermal power production. Toward that end, this report is organized as follows. Section 2 describes the methodology; Section 3 assesses the operations and maintenance (O&M) and decommissioning stages of the power plant life cycles; Section 4 provides LCA metrics for 20 new geothermal scenarios; Section 5 discusses an LCA model for well field exploration; Section 6 contains updated information on GHG emissions from geothermal power plants;

Section 7 provides a final comparison of geothermal power with other power generating technologies; and finally, Section 8 gives our conclusions. Detailed analyses and data and additional information are presented in Appendix A.

This page intentionally blank.

2 METHOD

Although the methodology we have used to conduct power plant LCAs is described in our earlier reports (Sullivan et al. 2010, 2011, 2012, 2013), for reader convenience, it is also discussed briefly here. Our approach to LCA involves process chain analyses (PCAs), in which all material and energy flows for specific and relevant processes associated with a product or service of interest are linked together to quantify overall system flows. This life cycle inventory (LCI) activity is the quantitative component of LCA. Information on conducting LCIs and other components of LCAs can be found in International Standards Organization sources (ISO 1997, 1998, 2000). A PCA strictly employs detailed, process-specific data that (ideally) are fully speciated in terms of purchased energy units (e.g., liters [L], kilowatt-hours [kWh], cubic meters [m^3], kilograms [kg], tonnes [metric tons or mt]), specific material consumption levels (e.g., tons, kg, mt), and amount of emissions (e.g., grams [g], kg). If such values for energy are not available, megajoule (MJ) or British thermal unit (Btu) values are acceptable, although they are less desirable due to ambiguities with regard to whether they represent high heat values or low heat values (LHVs) and whether they are life cycle values or purchased-energy values. All energy values employed herein are LHVs.

For the plant cycle (pc) stage, the materials that are tracked are concrete, steel, aluminum, copper, glass, silicon, iron, and plastics, which are needed for making plant buildings, wells, enclosures, and equipment (such as turbines, generators, and heat exchangers). Also tracked are fuels needed for on-site construction activities. For each scenario, plant performance characteristics (e.g., capacity, capacity factor, lifetime) are also specified. Sources of data are given in our earlier reports (Sullivan et al. 2010, 2011, 2012, 2013). The data on material composition and fuel use were subsequently normalized on a per-megawatt (MW) output capacity and are referred to as material-to-power ratios (MPRs). For solid materials, the unit of measure used is mt (tonnes) per MW of output capacity; for liquids, the unit is m^3 per MW. The MPRs can be thought of as metrics based on a "hardware functional unit" (i.e., an amount per MW of output capacity).

The MPRs were computed in a straightforward manner on the basis of facility material requirements divided by plant output capacity. Whether a plant is powered by coal, natural gas, nuclear, geothermal, or some other power source, its capacity is typically based on a single output (i.e., MW of electric power or MW_{el}). For plants with two outputs, such as geopressured gas and electricity (GPGE) facilities, there are two energy output flows: electric power (MW_{el}) and a natural gas production rate (MW thermal or MW_{th}). The sum of the two is the facility output capacity (i.e., MW mixed or MW_{mx}). In cases where natural gas produced from GPGE facilities is burned on site to produce electricity, the output is solely electricity (i.e., MW_{el}) — the sum of generation from both geofluids and gas.

Combining values for plant capacity, lifetime, and capacity factor with facility MPRs and the fuels used and emissions incurred during the production of those materials (GREET2 2012) yields two important service functional units for the plant cycle (pc) stage. They are the energy ratio ($\mathcal{E}_{pc} = E_{pc}/E_{out}$) and the CO_2-equivalent specific GHG emissions metric ($ghg_{pc} = \Sigma GHG_i/E_{out}$). In the ratio, E_{pc} and E_{out} are the pc fossil energy used and the total plant lifetime

electricity delivered, respectively. The emissions metric is a sum over a number of GHGs in terms of their CO_2-equivalent emissions (GHG_j). In addition to CO_2, the emissions of most significance here are CH_4 and N_2O. Values for $\mathcal{E}_{pc}$ and ghg_{pc} were estimated for the geothermal technologies and then compared with those for other renewable and fossil technologies.

The system boundary for our study is depicted in Figure 1; the product is the lifetime of kilowatt-hours of electricity at the wall outlet, unless stated otherwise. The life cycle stages explicitly shown in Figure 1 are the fuel cycle (fc) and plant cycle (pc). As pointed out above, the sum of pc and fc fossil energy and GHG ratios, respectively, provided estimates of $\mathcal{E}_{tot}$ and ghg_{tot} shown in previous work (Sullivan et al. 2010, 2011, 2012, 2013). However, omitted from the figure and our previous estimates of $\mathcal{E}_{tot}$ and ghg_{tot} were contributions from noncombustion O&M and plant decommissioning (dcm) activities, both of which are life cycle stages that were originally considered negligible. When those stages are formally accounted for and added to the fc and pc stages, the ratios become:

$$ghg_{tot} = ghg_{fp} + ghg_{fu} + ghg_{pc} + ghg_{o\&m} + ghg_{dcm} \quad (1)$$

$$\mathcal{E}_{tot} = \mathcal{E}_{fp} + \mathcal{E}_{fu} + \mathcal{E}_{pc} + \mathcal{E}_{o\&m} + \mathcal{E}_{dcm} \quad (2)$$

The question at hand is whether the corresponding energy and GHG ratios for the O&M and dcm stages are indeed negligible. The last three terms on the right side of both equations are termed the infrastructure cycle; their sums are ghg_{inf} and $\mathcal{E}_{inf}$, respectively.

These two metrics ($\mathcal{E}_{tot}$ and ghg_{tot}) are suitable for comparing the environmental performance of various power production technologies. To address current concerns about fossil fuel consumption, E_j (the numerator in $\mathcal{E}_j$) for any life cycle stage "j" in this analysis represents the sum of fossil energies only.

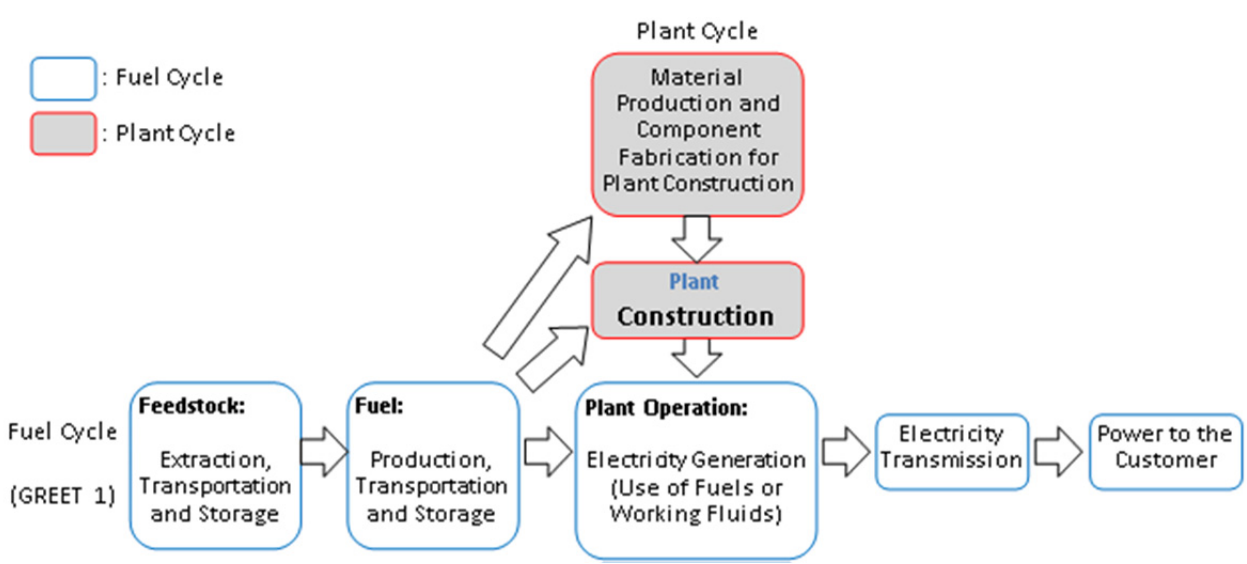

FIGURE 1 System Boundary for GREET Electricity Modules

3 ASSESSMENT OF THE OPERATIONS AND MAINTENANCE STAGE AND DECOMMISSIONING STAGE OF THE LIFE CYCLE ANALYSIS

The objective of Section 3 is to complete the "infrastructure" component of power plant LCAs. As stated previously, this component of the life cycle includes the pc, O&M, and dcm stages. In earlier work (Sullivan et al. 2010, 2011, 2012, 2013), we estimated only the $\mathcal{E}_{pc}$ and ghg_{pc} components of $\mathcal{E}_{inf}$ and ghg_{inf}, respectively, for power plants. Here, we estimate values for the O&M and dcm stages and assess their significance on $\mathcal{E}_{tot}$ and ghg_{tot} for geothermal, other renewable, and fossil power production technologies. Note O&M burdens as treated here do not include emissions arising directly from the combustion of fuel to produce electricity (e.g., those from burning coal to produce electricity). Those burdens are accounted for in the fuel use (fu) stage.

Unfortunately, there is comparatively little information in the literature that would provide meaningful inputs for LCAs in terms of materials and energy consumed during the O&M and dcm stages of power plant life cycles. Most of the studies that we found that addressed O&M and dcm focused on cost and, as such, lacked useful data on materials and fuels for these life cycle stages. For readers interested in power plant capital, fuel, and O&M costs, we suggest the following references: McNerney et al. (2011), "Updated Capital Costs" in EIA (2010b), Sargent and Lundy (2009), and Koomey and Hultman (2007). McNerney et al. (2011) points out that getting reliable data for power plant O&M has been difficult historically.

3.1 PREVIOUS ESTIMATES OF O&M AND DECOMMISSIONING VALUES FOR FOSSIL ENERGY CONSUMPTION AND GHG EMISSIONS

Some early work in this area was done by White and Kulcinski (1998); a selection of their results is shown in Table 1. Their paper reported energy and GHG ratios for the pc and O&M life cycle stages for nuclear fission, coal, wind, and fusion power plants. Table 1 also shows $\mathcal{E}_{pc}$ and ghg_{pc} values previously developed by us (Sullivan et al. 2010). Our values are two or more times less than the values reported by White and Kulcinski.

TABLE 1 Energy and GHG Ratios from White and Kulcinski (1998) for Plant Cycle, O&M, and Decommissioning Stages

Power Plant	$\mathcal{E}_{pc}$	Argonne[a] $\mathcal{E}_{pc}$	$\mathcal{E}_{o\&m}$	$\mathcal{E}_{dcm}$	ghg_{pc}	Argonne[a] ghg_{pc}	$ghg_{o\&m}$	ghg_{dcm}
Coal	0.005	0.002	0.014	3.2×10^{-4}	1.3	0.69	[b]	0.1
Nuclear fission	0.006	0.0012	0.008	6.0×10^{-4}	1.9	0.57	2.2	0.01
Wind	0.028	0.025	0.016	1.6×10^{-3}	10.2	8.9	4.0	0.4

[a] Argonne data from Sullivan et al. (2010) (shaded columns) were added for comparison.
[b] White and Kulcinski (1998) did not separate combustion-related GHGs from those of other O&M activities.

The White and Kulcinski values are based on a hybrid economic input output (EIO) method that blends PCA with EIO for those stages where PCA information is not available. It is their EIO estimate for plant construction activities that raises their $\mathcal{E}_{pc}$ and ghg_{pc} values so much higher than ours (Sullivan et al. 2010) shown in the Table 1. In fact, 90% of our $\mathcal{E}_{pc}$ and ghg_{pc} values arise from plant material production, and, as such, they are very much in line with the plant material production values given by White and Kulcinski (1998) (i.e., $\mathcal{E}$ = 0.002, 0.002, and 0.021 and ghg = 0.6, 0.7, and 8.6 for coal, nuclear, and wind, respectively).

Despite the differences between White's and Kulcinski's 1998 and our 2010 results, we chose to use their results to estimate the "relative" contributions of O&M and dcm to the total energy and GHG ratios. We did this for consistency purposes, because their approach is hybrid EIO for both pc and O&M, whereas ours is strictly PCA for only the pc. As Table 1 shows, their $\mathcal{E}_{o\&m}$ and $ghg_{o\&m}$ values are generally on the same order of magnitude as $\mathcal{E}_{pc}$ and ghg_{pc}. On the other hand, their dcm ratios are one or more orders of magnitude lower than the ratios of their pc counterparts.

In practice, the EIO method is based on using economy-wide economic data from more than 500 industrial sectors. That data can be related to the energy and emissions (Lave et al. 1995) associated with those sectors, and, as such, results from EIO analyses provide estimates of energy and emissions for a much larger system than that considered in the PCA. In fact, Beerten et al. (2009) noted in a recent review of three LCA studies on nuclear power that EIO and hybrid EIO results for nuclear power are significantly higher than the corresponding metrics in a PCA study for the same system. They attributed the difference between the PCA and EIO results to truncated system boundaries for PCAs relative to EIO analyses, to different study scopes, and to the high safety and regulatory costs associated with nuclear plants.

The system boundaries for an EIO analysis are much larger than those for a PCA, and EIO analyses are thus less illuminating for any specific industry (e.g., aluminum production). EIO analysis results are, in turn, less useful for environmental improvement initiatives, which is the primary motive for LCA in the first place. It is for this reason that our approach is PCA.

Others have also estimated the various life cycle stages, including O&M for nuclear power. Fthenakis and Kim (2007) used EIO analysis to estimate $ghg_{o\&m}$ for nuclear power and found it to range from 2.5 to 10.8 g/kWh. Given the typical variation in results between life cycle studies, this range is reasonably consistent with the White and Kulcinski (1998) results in Table 1. Much earlier, Tsoulfanidis (1981) and Rotty et al. (1975) had also computed energy ratios for nuclear power by using EIO tables. Their values (not shown) for pc are comparable to the White and Kulcinski values shown in Table 1.

Because dcm values shown in Table 1 are an order of magnitude less than either of their O&M and pc counterparts, we conclude that dcm makes negligible contributions to $\mathcal{E}_{inf}$ and ghg_{inf} and, hence, $\mathcal{E}_{tot}$ and ghg_{tot}, respectively. This conclusion is supported by recent results in Beerten et al. (2009), which showed that the contribution from the dcm stage for nuclear power can range from 3% to 7% of ghg_{inf} and $\mathcal{E}_{inf}$. As a result of this finding, the dcm stage is no longer considered in this report. Further, our decision is especially justified for fossil and nuclear power technologies, because our earlier results (Sullivan et al. 2010, 2011) showed that the pc stage

metrics are a fraction of a percent of ghg_{tot} and $\mathcal{E}_{tot}$; therefore, the dcm stage must be even smaller yet.

3.2 O&M LCA ESTIMATES FOR POWER GENERATING TECHNOLOGIES

O&M activities at a power plant involve the materials and energy needed for routine operation of the facility and the replacement parts, components, and materials needed for routine maintenance over the lifetime of the plant. The former represent variable operational burdens, and the latter represent fixed burdens. Their sum constitutes the total O&M life cycle burden for the plant. Although (as noted previously) the literature is much richer with regard to cost breakdowns of O&M, we found some information that was useful for our LCA. On the other hand, some O&M estimates were only available via modeling. Both are included in this study.

A summary of our PCA LCA results that quantify O&M life cycle burdens are shown in Figures 2 and 3; numerical values appear in Table A-1 of the appendix. The values shown in the figures are ghg_{inf} and $\mathcal{E}_{inf}$. The two significant components of the infrastructure stage are pc and O&M; as already stated, dcm, the third component, is considered negligible. The values in the figures are based both on specific information found in cited references and on the assumption that 10% of some plant materials are replaced over the plant's lifetime (Table A-1 has details). Values for pc given in this table can be found in Sullivan et al. (2010, 2011). The power generating technologies shown in the figures are three types of subcritical pulverized coal, NGCC, nuclear (average of boiling and pressurized water reactors), wind, PV, and three geothermal (EGS-B, HT-F, HT-B) technologies.

3.2.1 O&M for Renewable Power Generating Technologies

The geothermal technologies covered in this section are EGS-B, HT-F, and HT-B. O&M activities for geothermal plants include turbine refurbishment, descaling of piping and wells, air quality control, water emissions control (where relevant), well replacement, repair and replacement of down hole pumps, and others. However, from an LCA point of view, we expect the materials and fuels needed to drill and install replacement wells to be the dominant contributors to O&M life cycle metrics. The primary reasons a well needs to be replaced are thermal drawdown, a decline in flow rate, or both (GETEM [2013] technical manual). Because we could not find any specific information on geothermal power plant O&M activities, we used a modeling approach to estimate $\boldsymbol{\mathcal{E}}_{o\&m}$ and $ghg_{o\&m}$. More specifically, we used a value of 2%/yr for the well replacement rate for geothermal fields (Table 4-1 in EPRI [1994]) to estimate that half of a plant's wells are replaced over a facility's 30-year lifetime. With regard to EGS-B and HT-F plants, $\boldsymbol{\mathcal{E}}_{o\&m}$ and $ghg_{o\&m}$ are about 25% of $\mathcal{E}_{inf}$ and ghg_{inf} (see Figures 2 and 3 and Table A-1). These two systems were assumed to have 6-km and 2.5-km wells, respectively. On the other hand, $\boldsymbol{\mathcal{E}}_{o\&m}$ and $ghg_{o\&m}$ for HT-B amount to only about 10% of $\mathcal{E}_{inf}$ and ghg_{inf}, a consequence of its much shallower wells (1 km). Incidentally, the geothermal pc metrics used for Figures 2 and 3 include updated estimates for well field exploration; details on that are provided in Section 5.

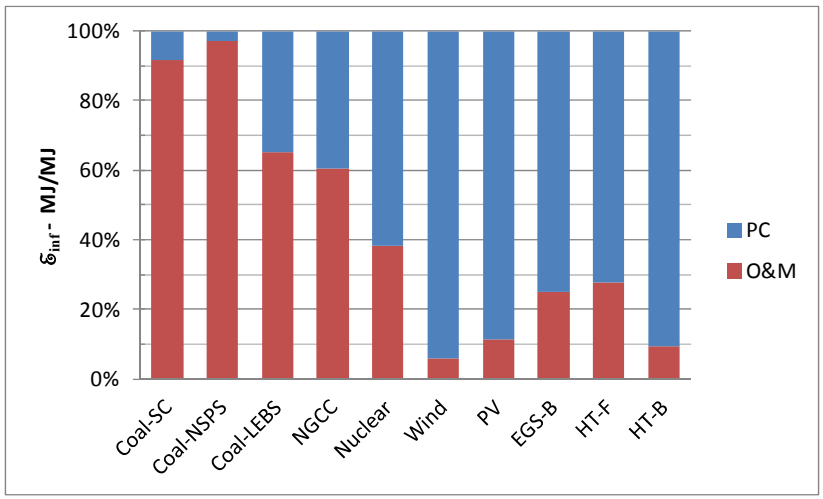

FIGURE 2 Infrastructure Energy Ratio Values on a Percentage Basis (Table A-1 provides numerical values and data sources)

For wind power production, we found the Vestas (2006) study to be quite comprehensive. However, very little attention was devoted to O&M in that study except for the replacement of half of a gearbox, which amounted to 6.3 mt of steel and 9 mt of iron per MW of capacity. Figures 2 and 3 show that $\mathcal{E}_{o\&m}$ and $ghg_{o\&m}$ for wind amount to only about 5% and 10%, respectively, of their $\mathcal{E}_{inf}$ and ghg_{inf} counterparts.

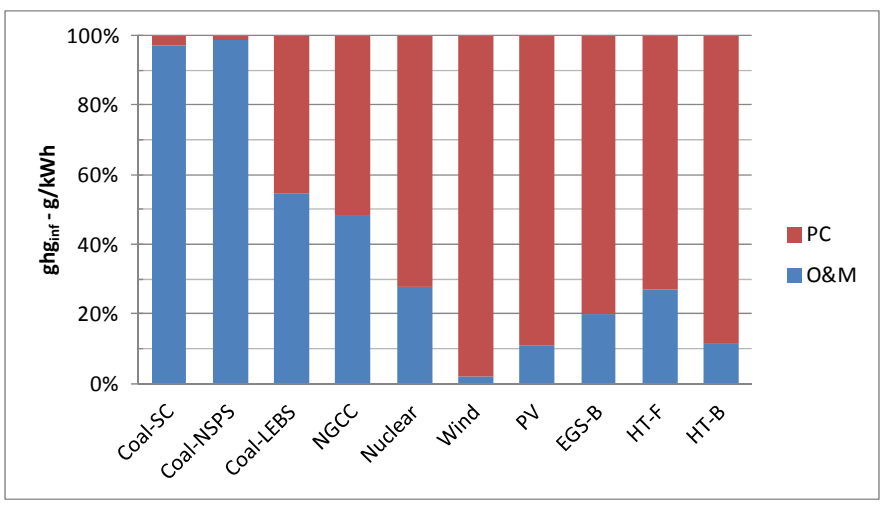

FIGURE 3 Infrastructure GHG Emission Rates on a Percentage Basis (Table A-1 provides numerical values and data sources)

Life cycle information on the O&M of PV facilities is also sparse. Because these facilities have few moving parts, one is inclined to conclude that O&M for them is quite limited. Some information was provided by Mason et al. (2006) on the heat and power that these facilities require to accommodate administrative, maintenance, and security staff, but these burdens are negligible. What does contribute more significantly to $\mathcal{E}_{o\&m}$ and $ghg_{o\&m}$ is the replacement of 10% of the plant's steel, aluminum, and silicon over its lifetime (Figures 2 and 3). Of the three materials, silicon dominates. Nevertheless, it is clear from the figures that PV O&M burdens amount to only 10% of their $\mathcal{E}_{inf}$ and ghg_{inf} counterparts. Other authors (Hsu et al. 2012; Frankl et al. 2006) also concluded that O&M life cycle burdens for PV systems are negligible.

3.2.2 O&M for Fossil Power Generating Technologies

Figures 2 and 3 show that for coal electrical power generation, $\mathcal{E}_{o\&m}$ and $ghg_{o\&m}$ represent the preponderance of their $\mathcal{E}_{inf}$ and ghg_{inf} counterparts. The importance of O&M for coal power is a consequence of the variable burdens associated with lime and limestone production; these materials are used for flue gas desulfurization (FGD). Sulfur gas emissions that result from coal combustion are significant and must be captured before flue gases are released to the atmosphere. All the coal scenarios in Table A-1 assume pulverized bituminous coal is used to fire the plants; the variation in results is due to the type of FGD technology employed. The first scenario is basically a subcritical (SC) U.S. base case, the second is an NSPS plant, and the last one is a high-efficiency (42%), low emission boiler system (LEBS) that employs a regenerative sulfur-capturing medium. (The references cited in Table A-1 have further details.)

Overall, $\mathcal{E}_{o\&m}$ and $ghg_{o\&m}$ values for coal plants are at least as large as the corresponding $\mathcal{E}_{pc}$ and ghg_{pc} values and generally much larger (between one and two orders of magnitude), depending on the FGD technology employed. Whether lime, limestone, or both are used, CO_2 is generated either during calcinations of limestone to lime or during the reaction of SO_2 with limestone during FGD.

The amount of sulfur gas [SO_x] formed during the production of electricity in natural-gas-fired plants is generally much less than it is in coal-fired plants. Before reaching the turbine, most of the sulfur in natural gas (mostly hydrogen sulfide [H_2S]) is routinely stripped with an amine process. In fact, NO_x emissions are of much more concern, and they are abated via selective catalytic reduction (SCR) using ammonia. In the one case shown in Figures 2 and 3 for NGCC, $\mathcal{E}_{o\&m}$ and $ghg_{o\&m}$ are about 60% and 50%, respectively, of their corresponding $\mathcal{E}_{inf}$ and ghg_{inf} values.

There is a dearth of information on the life cycle O&M burdens for nuclear power plants. Figures 2 and 3 and Table A-1 clearly show that our estimated $\mathcal{E}_{o\&m}$ and $ghg_{o\&m}$ values are roughly 33% of their $\mathcal{E}_{inf}$ and ghg_{inf} counterparts. This is somewhat surprising because it is often thought that spent nuclear fuel storage (an O&M component) would be quite burdensome from an energy and CO_2 emissions point of view. Table 2 compares our values for the O&M, pc, and fuel production stage (Sullivan et al. 2011) with values from a Swedish nuclear industry study (Vattenfall 2010). Overall, given the range of results typically extracted from different life cycle

studies, there is reasonable accord between the two sets of results. However, boundaries of the life cycle stages in the two studies are not exactly the same. For example, values for the Vattenfall (2010) pc stage shown in the table (a stage they refer to as "core-infrastructure") include not just plant construction but also decommissioning of the plant and spent fuel storage facilities. Vattenfall's "core" stage, which we consider part of O&M, accounts for the operation of the plant and management of spent fuel.

TABLE 2 Comparison of Fossil Energy and GHG Ratios Estimated by Argonne (Sullivan et al. 2011) with Results from the Literature (Vattenfall 2010)

Source	Fossil Energy Ratios			GHG Ratios (g/kWh)		
	$\mathcal{E}_{pc}$	$\mathcal{E}_{o\&m}$	$\mathcal{E}_{fp}$	ghg_{pc}	$ghg_{o\&m}$	ghg_{fp}
Vattenfall (2010)	0.0018	0.0008	0.015	0.72	0.33	4.6
Sullivan et al. (2011)	0.0014	0.0009	0.037	0.59	0.23	9.9[a]

[a] From GREET1 (2012).

3.3 KEY FINDINGS ABOUT POWER PLANT O&M BURDENS

From the results just presented on the O&M and dcm life cycle burdens of $\mathcal{E}_{inf}$ and ghg_{inf}, we identified a number of key findings:

- Despite being based on limited information, we conclude that dcm life cycle burdens are negligible.
- The O&M component of $\mathcal{E}_{inf}$ and ghg_{inf} ranges widely depending on the power plant technology used; it ranges from 95% or more for some coal plants to as little as a few percent for PV.
- For geothermal technology, the percentages are 20% for EGS-B with 6-km wells, 30% for HT-F plants with 2.5-km wells, and 10% for HT-B plants with 1-km wells.

Estimates of O&M burdens for geothermal plants were based solely on well replacements over a facility's lifetime. For the other plants, estimates of O&M burdens were based on the percentage of plant materials that are replaced over a facility's lifetime and, when appropriate, the materials needed for emissions abatement. The high percentages for coal plants are due to FGD, a variable burden incurred for every kilowatt of electricity produced.

4 ALTERNATIVE SCENARIOS FOR GEOTHERMAL POWER PRODUCTION

In a series of reports (Sullivan et al. 2010, 2011, 2012, 2013), we analyzed geothermal power production for five different scenarios. The systems analyzed were EGS, HT-F, HT-B, and GPGE for both greenfield sites (GPGE-gf) sites and reworked gas field sites (GPGE-rw). Details on the scenarios are provided in Table 3. The data from the analyses were used to develop plant, well, and plant-to-well models that generated the amounts of materials and fuels required to build those power plants. This section of the report discusses how we used our previously developed models (Sullivan et al. 2010, 2011, 2012) to explore the impact of a technology's maturity (current = "reference" versus future = "improved") on the life cycle metrics of $\mathcal{E}_{pc}$ and ghg_{pc} for a set of geothermal resources. Levelized cost of electricity (LCOE) results are also discussed.

TABLE 3 Details on Geothermal Scenarios Previously Analyzed (Sullivan et al. 2010)

	Scenario				
Parameter	1	2	3	4	5
Type of geothermal technology	EGS-B	HT-B	HT-F	GPGE-gf	GPGE-rw
Net power output (MW)	20	10	50		
Production-to-injection ratio	2	3 or 2	3 or 2	2	3
Ave. no. production wells	6.4±3.5	3.1±0.9	14.6±4.6	2	2
Number of turbines	Single	Single	Multiple	1	1
Type of generator	Binary	Binary	Flash	Binary	Binary
Type of cooling a	Air	Air	Evaporative	Air	Air
Temperature (°C)	150–225	150–185	175–300	130–150	150
Flow rate (kg/s)	30–90	60–120	40–100	35–55	27–47
Thermal drawdown (%/yr)	0.3	0.4–0.5	0.4–0.5	0	0
No. of wells replaced	1	1	1	0	0
No. of exploration wells	1	1	1	0	0
Production well depth (km)	4–6	<2	1.5 to <3	4, 5, 6	4, 5, 6
Injection well depth (km)	4–6	<2	1.5 to <3	2, 2.5, 3	2, 2.5, 3
Type of injection pumps	Surface	Surface	Surface	Surface	Surface
Type of production pumps	Submersible 3 km	Lineshaft or submersible	None	NA[a]	NA
Distance between wells (m)	600–1,000	800–1,600	800–1,600	NA	NA
Location of plant[b] re: wells	Central	Central	Central	Central	Central
U.S. geographic location	Southwest	Southwest	Southwest	Gulf Coast	Gulf Coast
Plant lifetime (yr)	30	30	30	30	30

[a] NA = not applicable.
[b] Location between production and injection wells.

4.1 NEW EGS, HT-F, AND HT-B SCENARIOS

Two cases (one "reference," one "improved") per geothermal technology were developed for each of 10 resource scenarios, resulting in a total of 20 new scenarios. Each reference/ improved pair representing one of four geothermal technologies (EGS-binary, EGS-flash, HT-B, HT-F) was applied to a resource normally exploited by that particular technology. The geothermal resources vary in depth, temperature, and geofluid flow rates typically encountered in fields used for geothermal power production. Details on those scenarios are provided in Tables A-2 and A-3. All reference cases are based on 2012 technology, whereas technologies representing the improved cases are projections into the future with implementation-ready dates of 2030 for EGS (Table A-2) and 2020 for hydrothermal (Table A-3).

All information in those tables was taken from a series of runs of the beta version of GETEM (2013). The primary purpose of the runs was to estimate reductions in LCOE that would be induced by improvements in geothermal technologies over their reference configurations for a range of geothermal resources. Parameters representing technology maturity included a plant's efficiency, capacity, and lifetime and the efficiency of exploration. For the five EGS resource scenarios appearing in Table A-2, well depths of 2, 2.5, 3, 3.5, and 4 km were assumed. Three of the EGS scenario pairs were for EGS-B; the remaining two pairs represent EGS-F. Well field parameters included well flow rates, resource temperature, resource depth, thermal drawdown rate, and financing alternatives (e.g., discount rate). Three HT-B alternative pair were explored at two depths, 1.5 and 2.5 km. Two HT-F scenarios were also studied at the same two depths.

When compared to our previous studies on geothermal power production (Sullivan et al. 2010, 2011, 2012, 2013), this alternative scenario set includes two unique scenarios. They are two EGS-F plants (Scenarios 4 and 5 in Table A-2). This was done in an attempt to explore the range of potential geothermal scenarios that might provide more attractive LCOE values.

4.2 RESULTS FOR NEW GEOTHERMAL SYSTEM SCENARIOS

On the basis of our previous plant and well models developed for this project (Sullivan et al. 2010, 2011, 2012, 2013), we estimated the material and fuel demands (measured as MPRs) for building the plants, aboveground piping, and wells defined for each scenario case. From these MPRs, corresponding values for $\mathcal{E}_{pc}$ and ghg_{pc} were subsequently computed. Note that both of these metrics represent the commitment of materials and fuels per unit of electricity output to build a power plant.

To facilitate the discussion of results in this section, here is the analytical form that represents our geothermal LCA models:

$$ghg_{pc} = \alpha/LT + [B * \gamma * N_I/2 + \beta * N_{tot} * f(d)]/[C * cf * LT] \quad (3)$$

where

α	=	a constant representing the sum of GHG emissions per MW of capacity from the fuels used to construct and produce materials for the plant, its equipment, and aboveground piping;
β	=	the sum of GHG emissions per unit of well depth that result from the fuels used to construct and produce materials for the wells;
γ	=	the GHG emissions per injection well that result from the fuel used for well stimulation;
f(d)	=	a function of depth;
C	=	the plant's capacity (MW);
cf	=	the capacity factor;
N_I and N_{tot}	=	the number of injection wells and total number of all wells, respectively;
B	=	a constant (0 for hydrothermal and 1 for EGS); and
LT	=	plant lifetime.

An expression of the same form can be written for $\mathcal{E}_{pc}$.

Figures 4 and 5 demonstrate the dependence of ghg_{pc} on the total length of wells in the field per MW capacity. (Table A-4 gives numerical values.) The figures illustrate that ghg_{pc} increases with increasing total length of wells per MW of capacity [N_{tot}(d/MW)], although some scenario pairs have lower ghg_{pc} values despite their higher N_{tot}d/MW values. However, this apparent contradiction is due to changes in β and γ coefficients in Equation 3 for different well depth regimes. The total length of wells includes lengths of injection, production, and exploration wells. Keep in mind that ghg_{pc} is contributed to by more than just well field materials production and drilling. As per Equation 3, it is also contributed to by materials for plants, the construction of plants, equipment, and aboveground piping between the wells and plant.

Another trend evident in Figure 4 is that all improved cases (open symbols) have lower ghg_{pc} values than their reference counterparts (filled symbols). The reason is that at the same resource depth, the improved cases require fewer wells per MW of capacity than do their reference counterparts. Also note that HT-F ghg_{pc} values are conspicuously lower than their HT-B counterparts. This difference arises from the α term in Equation 3 and is primarily due to the high material demand for air cooling systems by binary plants versus the much lower material demand for wet cooling by flash technology.

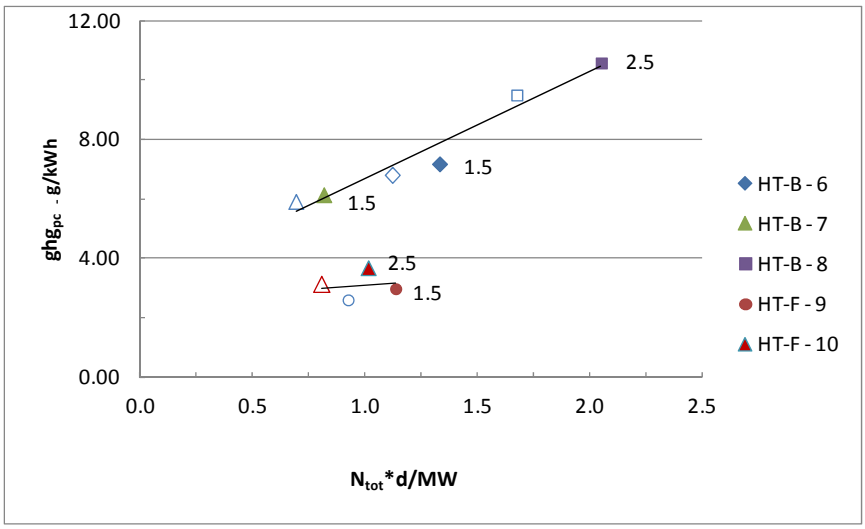

FIGURE 4 Hydrothermal Plant Cycle GHG Emissions (g/kWh) Versus Total Length of Wells per Megawatt of Capacity for Binary and Flash Scenarios (filled symbol = reference case, corresponding open symbol = improved case; postscript number = scenario ID, number next to the reference of each scenario pair = well depth [km])

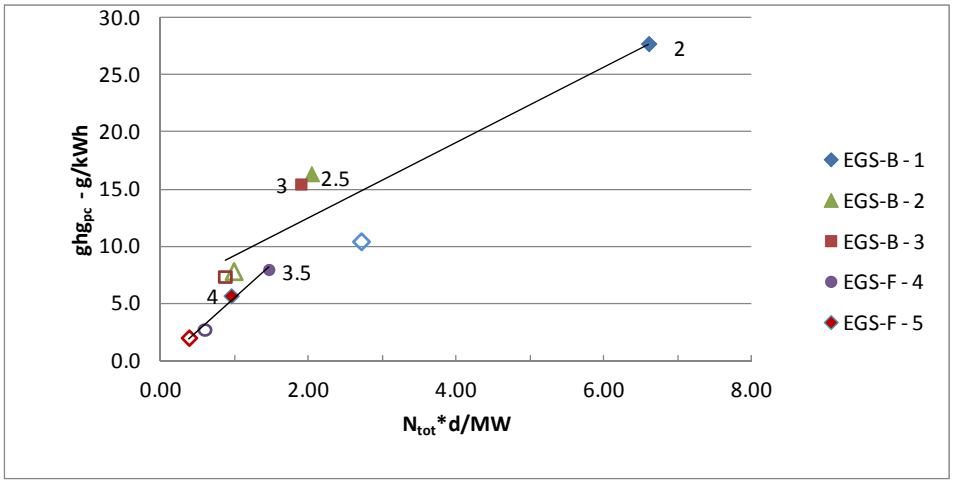

FIGURE 5 EGS Plant Cycle GHG Emissions (g/kWh) Versus Total Length of Wells per Megawatt of Capacity for Binary and Flash Scenarios (postscript number = scenario ID; filled symbol = reference case, corresponding open symbol = improved case; number next to the reference of each scenario pair = well depth [km])

Each ghg_{pc} value shown in the figures represents a geothermal plant with a specific capacity, well depth, number of wells, resource temperature, and flow rate (see Tables A-2 and A-3). This approach is a departure from our previous approach for specifying a geothermal scenario (in which each value represented a plant scenario with a specific power output at a fixed well depth but was averaged over a range of resource temperatures and flow rates (see Table 1) and, hence, number of wells.

Figure 5 shows ghg_{pc} values for the alternative EGS scenarios. Again, as was the case for the hydrothermal systems, all improved cases have ghg_{pc} values that are lower than their corresponding reference case values. However, the reductions in ghg_{pc} for the improved cases from their reference counterparts are much greater for EGS than for the HT scenario pairs. There are two reasons for this. Relative to their reference counterparts, the improved EGS cases have (1) much shorter well lengths per MW of capacity and (2) plant lifetimes (LTs) of 30 years (versus 20 years for the reference cases). The impact of a plant's lifetime on ghg_{pc} is evident in Equation 3. As is the case for the HT scenarios, ghg_{pc} values for EGS-F plants are lower than those for EGS-B plants (see Figure 4). The reason is the lower material demand of the EGS-F wet-cooling systems.

The new EGS-B scenarios assume wells are 2 to 3-km deep (see Table A-3), much shallower than the 4 to 6 km assumed for the wells before (Sullivan et al. 2010, 2011) for greenfield "deep EGS" sites. The shallower EGS-B scenarios can be thought of as approximations of "near field" EGS and, as such, are representative of areas near existing HT-B fields where low permeability and fluid availability might be enhanced enough by EGS field stimulation methods to bring the wells into production. A more complete discussion of this type of EGS can be found elsewhere (Augustine and Young 2010; Clark et al. 2012).

LCOE and ghg_{pc} results for the 10 scenario pairs are compared in Figures A-1 and A-2; Table A-4 has the values. The figures show that within technology classes (HT-B, EGS-F, etc.) and within cases (reference and improved), both LCOE and ghg_{pc} trend the same way from scenario to scenario. In other words, when LCOE either increases or decreases, ghg_{pc} does the same. For example, in Figure A-2, both LCOE and ghg_{pc} values for HT-B reference cases decrease from Scenario 6 to 7 and then increase from Scenario 7 to 8. The same correlations hold for the improved HT-B scenarios as well as LCOE and ghg_{pc} results for HT-F, EGS-B, and EGS-F (also shown in Figures A-1 and A-2). These trends are expected. Both LCOE and ghg_{pc} depend on a number of factors, but a significant one is the sum of the lengths of all wells per megawatt of capacity (N * d/MW). In short, as more materials and fuels are needed for a well field, both LCOE and ghg_{pc} are expected to increase, and as Table A-4 shows, when N * d/MW increases or decreases, both the LCOE and ghg_{pc} values within scenario pairs follow suit.

Two other important trends are revealed in Figures A-1 and A-2. First, the improved cases always have lower LCOE values than their reference counterparts for both the EGS and HT scenarios. In fact, as Tables A-2 and A-3 show, LCOE values for improved EGS cases are a third to a fourth of their reference counterparts and, in the case of HT, about half of their reference counterparts. Second, LCOE reductions imparted by the improved cases over their corresponding reference cases are conspicuously larger for the EGS scenarios than for the

hydrothermal scenarios. The reasons for both of these trends are the same as those just discussed for ghg_{pc} reductions.

Although we have not plotted any of the $\mathcal{E}_{pc}$ data, values for them appear in Table A-4. As expected, they trend with regard to the total length of wells in very much the same way as does ghg_{pc}.

4.3 RESULTS ON A CAPACITY BASIS

Another way to look at these results is on a MW of capacity basis; values for this metric are shown in Figure 6. Despite the wide variation of results shown in the figure, important trends can be noted. First, as capacity increases, ghg_{pc} decreases; it apparently approaches a lower limit at higher capacities. This trend is likely due to an economy-of-scale effect. Further, despite the wells being progressively deeper, the results from alternative EGS-B scenarios seen in Figure 6 for both 20-year (reference cases) and 30-year (improved cases) facility lifetimes clearly show a significant dropoff in ghg_{pc} values with an increase in plant capacity. This is due to progressively higher resource temperatures with depth (see Tables A-2 and A-3). On the other hand, EGS-B results from our previous work (Sullivan et al. 2012) (see values labeled "prv" in Figure 6) clearly demonstrate that at fixed capacity, ghg_{pc} increases with increasing well depth. All of these trends arise from the β term in Equation 3. Also note that EGS-B facilities have higher ghg_{pc} values than do their EGS-F counterparts. This is primarily the result of the greater total length of all wells ($N_{tot}d$/MW) required to deliver adequate thermal energy from lower-temperature reservoirs to the plant. Figure 6 also shows that the ghg_{pc} of the improved case is lower than that of its reference counterpart for all EGS scenario pairs. This situation arises from both the plant's lifetime and its capacity.

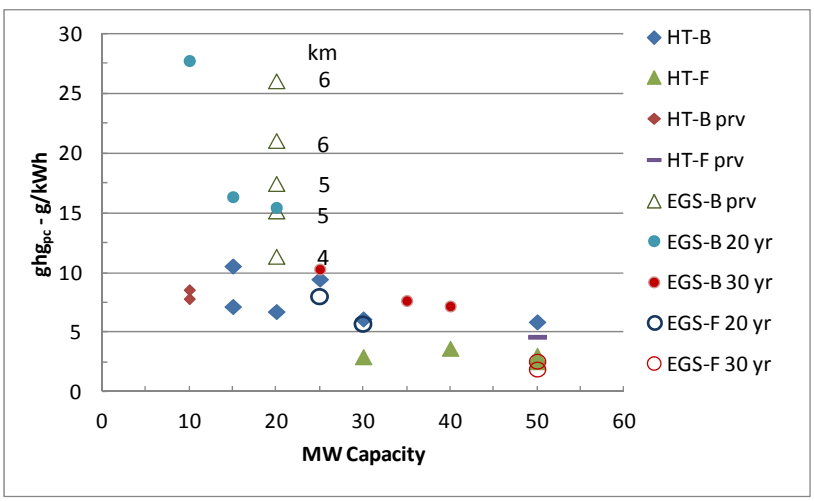

FIGURE 6 Plant Cycle GHG Emissions (g/kWh) Versus Plant Capacity for the Geothermal Power Production Scenarios Listed in Legend (postscript prv = results from previous study [Sullivan et al. 2012]; well depths are included for EGS-B base scenarios)

The results presented in this section include the contribution from well field exploration (computed either per Section 5 or per GETEM [2013]). Our estimates of the plant cycle stage of geothermal power production now is now complete and include values from exploration, well field development, plant construction, and above ground piping.

4.4 KEY FINDINGS FROM THE ANALYSIS ALTERNATIVE GEOTHERMAL PLANT SCENARIOS

Key results from a set of 10 pairs of reference versus improved scenarios of flash and binary hydrothermal and EGS plants evaluated by using our geothermal models follow here:

- The improved cases for all EGS and HT scenarios yielded $\mathcal{E}_{pc}$ and ghg_{pc} values lower than those of their reference counterparts and, as such, are consistent with improved versus reference LCOE results derived from GETEM (2013).

- The values of ghg_{pc} for the alternative scenarios fall into the same range as results published previously (Sullivan et al. 2010, 2011, 2012, 2013) for EGS-B, HT-F, and HT-B.

- The values of ghg_{pc} for geothermal binary plants in the alternative scenarios range from about 6 to more than 25 g/kWh; the range is 2 to 8 g/kWh for the alternative EGS-F and HT-F plant scenarios.

The lower values of $\mathcal{E}_{pc}$, ghg_{pc}, and LCOE for the improved cases relative to those of their reference case counterparts are due to decreases in the total length of wells per MW of capacity. The GETEM runs for the 20 new scenarios (10 scenario pairs) were part of a study to identify ways to reduce LCOE in each scenario pair. In fact, LCOE values for improved EGS cases are a third to a fourth of the values for their reference case counterparts. For HT technologies, improved case LCOEs are about half of those of their corresponding reference cases.

This page intentionally blank.

5 GEOTHERMAL EXPLORATION

A significant amount of exploration and development must be conducted before a geothermal power plant can be brought on line (commissioned). The important stages of this process include well field exploration, well field development, plant construction, and, finally, site operation. Ultimately, wells need to be drilled into a geothermal resource before a geofluid can be brought to the surface to produce power. Because drilling wells at a potential geothermal site is an expensive undertaking, a developer must be convinced that a viable fluid resource is present before starting. In fact, Jennejohn (2009) estimated that the exploration stage can represent as much as 42% of overall project costs. Hence, exploration procedures have evolved to increase the success rate in developing geothermal resources. Such procedures can be divided into two critical groups: predrilling and drilling. Predrilling activities employ geoscientific methods to identify promising locations and assess their potential as commercially viable geothermal resources. The methods used include remote sensing and various other geophysical and geochemical surveys, which provide data that are used to develop a preliminary model of a potentially commercial resource. For LCA purposes, we define exploration drilling as the drilling activities conducted before site commissioning. It involves drilling of thermal gradient holes (TGHs), core holes, and slim holes and, finally, confirmation wells. Except for confirmation well drilling, the exploration drilling activities are considered site surveying methods, from which the resultant information, when combined with information from geoscientific methods, further refines the model of the resource and guides decisions on the next steps to be taken. The drilling of production and injection wells is not considered part of the exploration stage but rather part of the well field development stage, which occurs after the presence of a commercial resource has been confirmed.

5.1 METHODS FOR GEOTHERMAL WELL FIELD EXPLORATION

Exploring for geothermal resources is a process in which the iterative application of geoscientific and drilling methods is used to determine the commercial viability of a site. Geoscientific methods employed for this purpose include the following:

- Remote sensing (e.g., hyperspectral, light and radar [LiDAR], and interferometer synthetic aperture radar [INSAR] techniques), which is used to look for encouraging surface features (heat flow, topography shifts);
- Geologic mapping;
- Geophysical assessments, which use gravitational, seismic, electrical, and magnetic methods;
- Geochemical analysis of site fluids;

- Petrological studies, used to look for heat-induced mineralization; and
- Geographic information system (GIS) analysis combined with modeling.

A more detailed discussion of these methods is beyond the scope of this study, but an overview of them can be found elsewhere (DOE 2010; OpenEI 2012). Exploration drilling methods can be used with TGHs; with core holes to determine the stratigraphy of site mineralogy; with slim holes (and core holes) equipped with a data logger to determine temperature, pressure, porosity, permeability, flow rates, and other measures; and with confirmation wells. From a material and drilling fuel point of view, confirmation wells are effectively production wells, and the methods that involve them are the most expensive.

Typically, the geoscientific and drilling methods are combined in such a way as to minimize cost and maximize useful information. Of course, the specific combination of these methods can vary from site to site. Because the presence and extent of a geothermal resource is difficult to "see" directly, the evolving array of data collected during the exploration process from the various geoscientific methods progressively refines the model of that resource, providing a clearer "picture" of it. Initially, the lowest-cost methods are applied, and the resulting data then inform decision makers on whether or not to proceed to the next step. If the decision is yes, additional investment is required, typically involving even more expensive methods, including well drilling. If, in the end, all results are sufficiently positive, confirmation well drilling commences, followed by long-term flow and temperature testing.

Despite their significant costs (but invaluable input for resource assessments), predrilling methods have a negligible impact on the total life-cycle results of geothermal power since they are analytical in nature. On the other hand, well drilling — with its associated needs for casings, cement, water, and fuel — has significant life cycle impacts that increase with the number of wells drilled. Because of the differences in material and fuel requirements between predrilling and drilling methods and the concomitant effects on exploration life cycle burdens, our focus here is on the drilling stage of geothermal well field exploration.

5.2 GEOTHERMAL WELL FIELD EXPLORATION STUDIES

Although exploration drilling is expected to add significantly to the life cycle burdens of geothermal power production, there is, unfortunately, little published information on the number of exploration wells needed to confirm the commercial viability of the geofluid resource. Sanyal and Morrow (2011) published a study on drilling success rates in the development and operational stages of existing geothermal fields (Geysers and Kamojang) but found little information to establish success rates for the exploration stage. On the other hand, a recent pair of studies published by Shevenell (2012a,b) sheds some light on exploration drilling requirements.

Figure 7, which uses results extracted from Shevenell (2012a,b), shows two distinct trends. The number of exploration wells needed to develop an operational facility averages about 55 wells on the high end and 12 on the low end, with a broad empty band in-between. Moreover,

each trend appears to be independent of both plant capacity and resource depth. The high range might be an anomaly, since it represents sites owned by multiple entities during the exploration period and before plant commissioning. In fact, Shevenell (2012a) suggests that the high range might have arisen because any one of the site owners either was not aware of or did not use the exploration results of previous owners. Thus the actual range of exploration drilling might be closer to that of the lower average. The results in Figure 7 are from a limited set of data that represent only the exploration drilling done in Nevada for nine currently operating geothermal power plants.

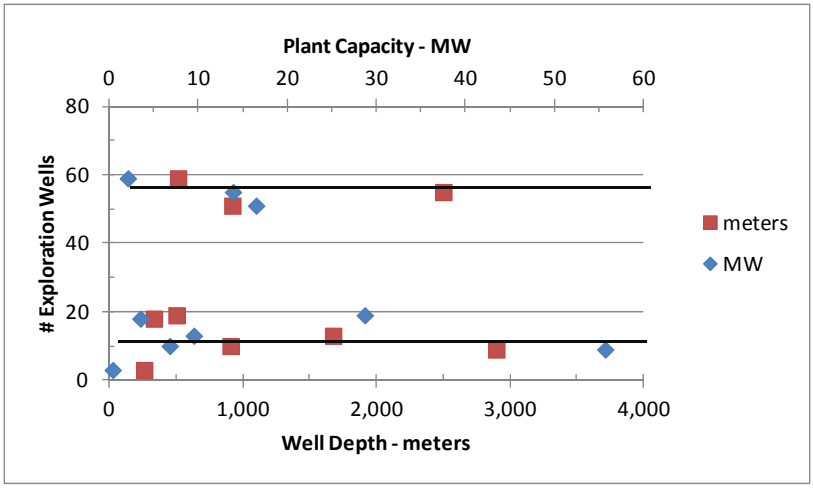

FIGURE 7 Dependencies of the Number of Exploration Wells Needed to Develop a Geothermal Plant on Plant Capacity and Resource Depth (dark horizontal lines are trend lines) (Data source: Shevenell 2012a,b)

Figure 8 shows that well field drilling costs increase with plant capacity (data from Shevenell [2012a,b]). In general, this trend is expected, since the use of more wells for a given resource implies greater capacity. However, drilling costs per plant capacity also depend on resource depth, temperature, and flow rates. Most of the drilling costs are associated with drilling costly production and injection wells; exploration drilling is generally much cheaper. Figure 8 also shows another expected trend: The number of production wells needed at the time of plant commissioning increases with plant capacity.

Often discussions are held about attaching a success rate to exploration drilling. However, both Shevenell (2012a,b) and Sanyal and Morrow (2011) concluded that it would be hard to do this. We, on the other hand, argue that exploration drilling, when skillfully applied, is always useful because it provides valuable information to decision makers, whether or not a viable resource is present.

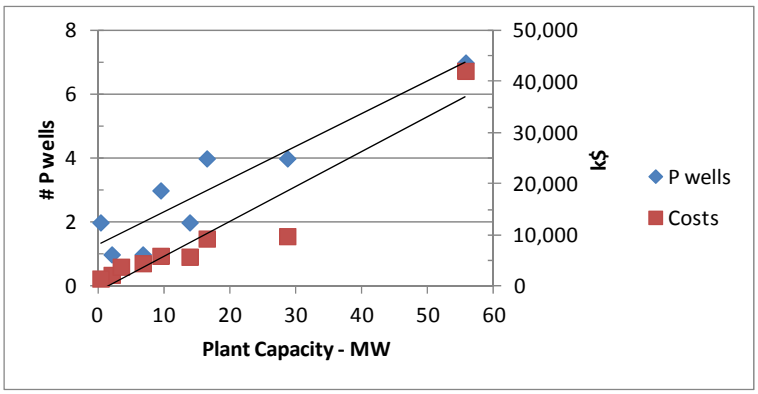

FIGURE 8 Well Field Drilling Cost and Number of Production Wells Versus Plant Capacity (MW) for Plants in Nevada (Data source: Shevenell 2012a,b)

5.3 EXPLORATION MODEL FOR GEOTHERMAL LIFE CYCLE ASSESSMENTS

To estimate the life cycle burdens for the exploration stage of geothermal power, we advance the following approach:

1. Use a variety of geochemical and geophysical methods to assess up to five sites that have some geothermal power potential.
   a. From these sites, identify three with the most potential.
   b. Drill five shallow and two deep core holes at each of the three sites.
2. From this set of sites, choose the one with the highest potential.
   a. At that site, drill a series of confirmation wells (configured as production wells). Attach a probability of success (P_1) to each confirmation well drilled. P_1 = the probability that a confirmation well meets both temperature and flow rate targets, especially after long-term testing.
   b. Declared the site a success if three of five confirmation wells are productive.

This approach is based on both industry input and the Shevenell (2012a,b) work.

The exploration drilling process is divided into two substages: survey drilling (slim holes, core holes, TGHs) and confirmation well drilling. Due to their comparable material and fuel requirements, core holes and slim holes are treated as being the same for LCA purposes. Because TGHs are typically drilled from the back of a truck, it is assumed that they have minor fuel requirements. Nevertheless, TGHs are an extremely valuable component of the subsurface survey by pointing to where core holes, slim holes, and confirmation wells should be drilled.

Because success is not guaranteed even after geoscientific and drilling surveys are conducted, a probability (P_1) is introduced to estimate the success rate for confirmation well drilling. To minimize costs and risks, five is assumed to be the maximum number of confirmation wells drilled per site. Overall, the model assumes that the amount of exploration drilling is independent of the output capacity of the final geothermal facility. In the scheme just described, 15 shallow core holes and 6 deep core holes are drilled per set of three sites explored.

The number of confirmation wells drilled at the high-potential site ranges from three to five. However, values for the number of survey and confirmation wells drilled over an ensemble of trials are needed to represent actual exploration practice. To represent such a population, we computed in a spreadsheet a site success rate based on an ensemble of 200 hypothetical sites, assuming a confirmation well success rate of P_1. From that model, the ensemble's average number of confirmation wells drilled per "successful site" and its corresponding standard deviation were derived. Given that the site's success rate depends on P_1, the model estimates that the total number of exploration wells/holes (confirmation plus survey) drilled per "successful" site ranges from 22 survey wells and 3.9 ±0.7 confirmation wells for $P_1 = 0.8$ to 30 survey wells and 5.9 ±0.7 confirmations wells for $P_1 = 0.6$. These values account for all exploration drilling of an ensemble of sets of three, including successful and unsuccessful triplets.

We further assumed that the three successful confirmation wells drilled on a successful site are later converted to production wells and, as such, are attributed to well field development and not exploration. All other confirmation wells (failed wells on either successful or unsuccessful sites and successful wells on failed sites) are considered failed confirmation wells and are attributed to the life cycle burdens of exploration.

A geothermal site is considered a success when the flow rate and temperature of the geofluid from its wells are sufficient to result in a commercially viable power plant (Sanyal and Morrow 2011). However, because success also depends on the local price for electricity and on well costs (which increase with depth), no attempt was made to define the flow rates and temperatures needed for success. Generally, values between 2 and 3 MW per production well (Sanyal and Morrow 2011) are thought to represent successful sites. In practice, however, the entity that is drilling the wells must be the judge of success. On the other hand, because our approach represents a surveying scheme (informed by industry input) with a statistical component, the output from our model provides estimates of life cycle well field exploration burdens per successful site that correspond to an ensemble of attempts to find commercial geothermal resources.

5.3.1 Well Assumptions

Based on Jennejohn (2009) and Benoit et al. (2005), we made the following assumptions about core holes: (1) A 6.75-in. core hole is bored to a depth of 25% of the total well depth, then cased with a 4.5-in. casing and cemented in place. (2) From there, a 3.83-in core hole is bored the rest of the way to the targeted depth. Our analysis counts cement, casings, diesel fuel, and water used for core and slim hole drilling as exploration life cycle burdens. The water required could be expensive if there is none or only a little available on site and it has to be trucked in. The core rod material is not considered an exploration life cycle burdens because it is assumed to be reusable. It is also assumed that the shallow holes are drilled to 50% of the resource depth, whereas deep holes go all the way to the resource. All core/slim holes are assumed to be cased to 25% of the targeted depth.

Diesel fuel requirements for core and slim hole drilling are based on the daily fuel consumption rate for a 300-hp drilling rig (200 gallons per day or gal/d) times the number of

days required to drill the core holes. Drilling rates for coring can range from 22 to 30 m/d (Benoit et al. 2005). For our modeling, we assumed 34 days per kilometer of depth (about 29 m/d). Water for core drilling is used for (1) the cement in the cased zone of the core hole and (2) the mud needed to cool the coring tool and to flush cuttings away. Based on industry practice for drilling rotary cone bits, the mud and hence the water requirements are typically about five times the bore volume, a value which we applied to both core holes and slim holes.

Because confirmation wells are intended to be production wells, we modeled them as the latter, using materials and fuels required for their construction found in our previous work (Sullivan et al. 2010, 2011). Based on the just-cited number of survey and confirmation wells and their corresponding material and fuel requirements, we computed the additional (exploration) amounts of cement, steel casing, water, and diesel fuel to be added to the geothermal facility's MPRs for plants, well field development, and plant-to-well piping.

5.4 EXPLORATION RESULTS

The following treatment estimates the contribution of well exploration to the life cycle material and fuel burdens for all well field activities. Estimates of the life cycle material and fuel burdens (MPRs) for all well field drilling were generated for EGS-B, HT-B, and HT-F facilities by using both our well field exploration and well field development models. The latter, developed to estimate the MPRs for production and injection wells, is described in Sullivan et al. (2010. 2011, 2012). A general expression representing our well field models is as follows:

$$MPR = [(N_P + N_I + N_{fc}) * MPW + N_{ch} * MPW' + N_I * M_{st}]/MW \quad (4)$$

where N_P and N_I = the number of production (P) and injection (I) wells, respectively, N_{fc} = the number of failed confirmation wells, N_{ch} = the number of core holes, M_{st} = the materials (diesel and water only) required for well field stimulation (valid only for EGS, zero otherwise), and MPW and MPW' = the amounts of material or fuel per P well hole and core hole, respectively, both of which depend on resource depth. The contribution of exploration to this expression is represented by the terms proportional to N_{fc} and N_{ch}. Results based on this expression are shown in Figure 9 for cement. Figures A-3, A-4, and A-5 have results for steel, diesel, and water, respectively. Values for data in the figures are provided in Table A-5. Each figure shows three well field MPR entries per technology: P/I denotes the sum of P wells and I wells only; P/I/1 denotes one additional P well added to the P/I sum; and P/I/Ex denotes the collective burdens from our exploration model (Ex) added to the P/I sum. The P/I/1 case represents our original attempt to account for exploration, which was by adding one additional P well to the operating P and I wells for the scenario.

As seen in the figures, exploration drilling activities for EGS-B as per our model (core/slim holes and confirmation wells) contribute appreciably to well field MPRs — certainly more than our original estimate of one extra production well. As expected from Equation 4, well field MPRs across all of the geothermal technologies show a clear dependence on well depth, most conspicuously so for EGS-B. In this case, the dependence becomes progressively higher

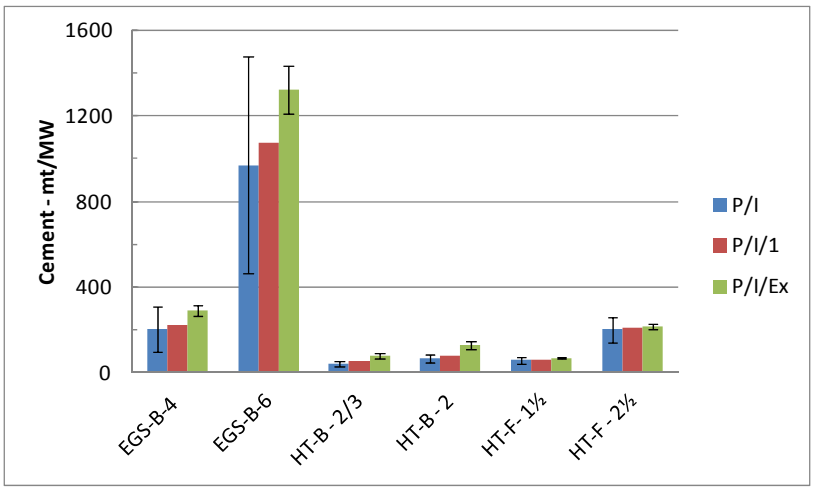

FIGURE 9 Cement MPRs (mt/MW) for Various Geothermal Technologies (postscript numbers = well depths [km]; error bars show ±1, representing well number variation for P/I and failed confirmation well variation for P/I/Ex; P_1 = 0.6)

with the addition of extra liners required at depths of 5 and 6 km. Of course, with regard to shallower (such as near or in-field) EGS wells, which are briefly discussed in Section 4, their MPRs (except for well field stimulation) tend to be like those of their HT-B and HT-F counterparts at comparable depths. For EGS-B facilities, the added steel and cement for exploration correspond to about 30% of their respective total well field MPRs. Also for EGS-B, exploration diesel amounts to about 45% of its well field MPR. Diesel required for well field stimulation has been estimated to be 118 m^3 per injection well, a value which is about 8% or less than the total well field MPR.

Figures 9, A-3, A-4, and A-5 and Table A-5 also include well field MPR data for HT-B technologies. Because of the shallower wells with single liners, MPRs for HT-B are considerably lower than MPRs for EGS-B. Nevertheless, the total MPRs for cement, steel, and diesel for HT-B have a higher relative contribution from exploration (around 50% for steel and cement, 70% for diesel, and 49% for water) than is the case for EGS-B. This is primarily because fewer production and injection wells ($N_P + N_I$; see Table A-5) are needed for the lower-capacity HT-B scenario. Given that our model (like the Shevenell data just discussed) has a fixed number of exploration wells (core holes, slim holes, and confirmation wells) plus or minus some variation for a plant of any capacity, the relative contribution of exploration to the total increases as ($N_P + N_I$) decreases. For the same reason, the relative contributions of exploration well activities to the various MRPs are quite small for HT-F. In this case, however, the HT-F plant, with its higher capacity (see Table A-5), has a larger number of production and injection wells to which a fixed number of exploration wells contributes comparatively less. Further the results in Table A-5 for HT-F show the contribution of exploration to the total MPRs is 17% for cement, steel, and water for wells that are 1.5-km deep and 7% for wells that are 2.5-km deep; for diesel plants, the exploration contribution is about 35%.

Well field water consumption values computed from our models account for drilling muds, well cement, and, in the case of EGS-B, well field stimulation. A comparison of well field water requirements among the technologies is shown in Figure A-5. (Table A-5 has numerical values.) Based on these results, the range of percentages of exploration water consumption to the corresponding totals are 14% to 22% for EGS-B with 4-km to 6-km wells, respectively; 12% to 17% for HT-F with 1.5-km to 2.5-km wells, respectively; and about 50% for HT-B with 2/3-km to 2-km wells. The figure clearly shows that well fields for EGS-B require significantly more water than well fields for either HT-F or HT-B plants. Even though in this case, the large difference is due to EGS-B's deep wells (greenfield sites) and stimulation, the difference would still occur (albeit it would be somewhat less) for shallower EGS well fields (near or in field sites) because of the magnitude of the stimulation water. As per a recent report by Clark et al. (2012), the value for EGS-B injection well stimulation used herein was 19,400 m^3 per injection well.

Although this amount of water consumption may appear to be quite large, in actuality, it is quite small when compared to operational water consumption. For example, adding well field drilling water consumption values in Table A-5 for the P/I/Ex scenarios to corresponding values for plant construction, which range from 14 to 40 m^3/MW, yields a lifetime electricity generation weighted water consumption rate that ranges from about 0.001 gal/kWh for HT-B and HT-F to about 0.009 gal/kWh for EGS. As pointed out in Clark et al. (2012) and Sullivan et al. (2013), operational water consumption can range from 20 times to more than 100 times more than it is for its $[H_2O]_{pc}$ counterparts. A more complete discussion of water use for geothermal plant and well construction and operations can be found in Sullivan et al. (2013) and Clark et al. (2012).

Two sets of range bars are also shown in Figures 9, A-3, A-4, and A-5. The set attached to the P/I bars are substantial and represent variations in the MPRs due to variations in the sum of N_P and N_I needed to deliver a specific amount of geofluid to achieve plant design capacity. This amount of geofluid, in turn, depends on resource temperatures, geofluid flow rates, and, in the case of EGS-B, submersible pumps. This was modeled in our earlier work (Sullivan et al. 2010, 2011) (see Table 3). The other set of range bars are attached to the P/I/Ex bars. They arise from the confirmation well success rate, P_1, which was assumed to be 60% for these figures. As expected, when P_1 is set to 80%, both the average number of confirmation wells drilled per successful site and its variation are reduced (see discussion in Section 5.3; also see Figure A-6). Upon comparing the two sets of range bars in Figures 9, A-3, A-4, and A-5, it is clear that the variation in the number of operational wells exceeds that associated with confirmation well drilling.

Figure 10 shows the amounts of cement required to build plants and well fields for each of the geothermal technologies covered herein. The figure shows that the production and injection wells are generally the largest consumers of cement for EGS-B and HT-F, whereas for HT-B, the largest consumer is plant construction. This is due to the comparatively shallow wells for the HT-B scenarios. For the purposes of this illustration, plant cement was computed to represent 20% of the concrete needed to build the aboveground facility, a percentage based on typical concrete recipes.

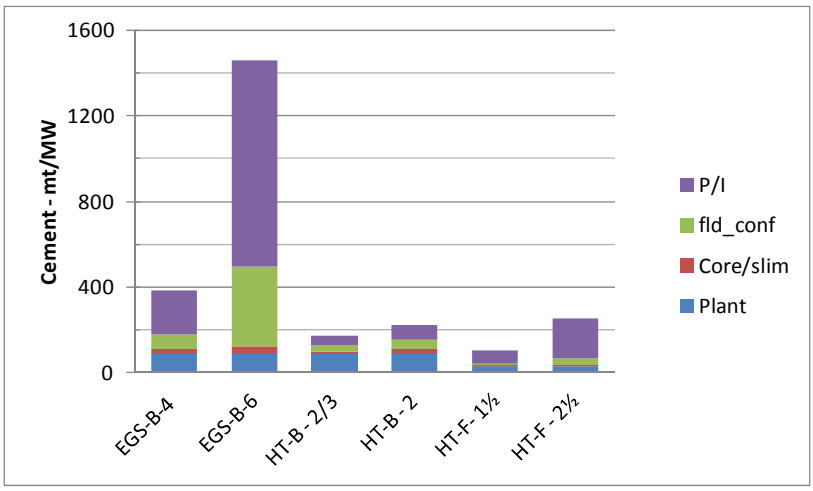

FIGURE 10 Amounts of Cement Needed to Build Power Plants and Well Fields (P_1 = 0.6)

Figures 11 and 12 show $\mathcal{E}_{pc}$ and ghg_{pc} values for the geothermal power systems covered herein. These plant cycle values were computed by using plant cycle MPR data, which represent fuels used for well drilling; plant construction; the installation of aboveground piping; and the production of materials used in plant structures, equipment, wells, and aboveground piping. As expected, the figures show increasing values of $\mathcal{E}_{pc}$ and ghg_{pc} with well depth. Moreover, the $\mathcal{E}_{pc}$ and ghg_{pc} values for EGS-B systems are considerably larger than are those for the HT-F plants. There are two reasons for this result. First, very large air-cooling structures were assumed for binary plant condensers, which represent about half of the plant's steel and concrete. Second, large amounts of cement, steel, and fuel are needed for drilling deep wells.

Another trend evident in Figures 11 and 12 is that $\mathcal{E}_{pc}$ and ghg_{pc} values for the HT-B plant are intermediate to those for EGS-B and HT-F technologies. This result was also expected. The HT-B system also uses air-cooling systems, but, at the same time, its wells are much shallower than those used for the EGS-B technology. Finally, for all but GPGE facilities, HT-F has the lowest $\mathcal{E}_{pc}$ and ghg_{pc} values. HT-F plants are typically water cooled, requiring smaller structures than do air coolers, and they have a comparatively high-power output due to generally higher resource temperatures.

We did not estimate life cycle exploration burdens for GPGE operations. With regard to green field sites, the burden would be consistent with natural gas exploration, for which we have no information. With regard to reworked sites, the resource has already been developed, albeit degraded by increased brine (geofluid) and reduced gas production. Hence, for the reworked sites, little (if any) additional exploration burden would need to be added. Nevertheless, as a point of reference, we included their $\mathcal{E}_{pc}$ and ghg_{pc} values (excluding exploration) in Figures 11 and 12. See Sullivan et al (2011) for a detailed discussion of GPGE systems.

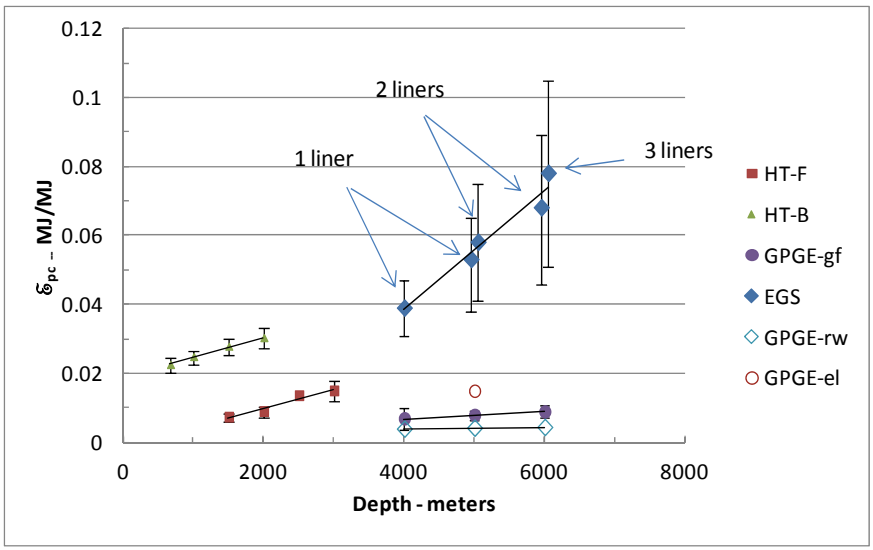

FIGURE 11 Plant Cycle Fossil Energy Ratios for Several Geothermal Energy Technologies (range bars represent 1 standard deviation of combined N_{P+I} and confirmation drilling variation) (Source: Sullivan et al. 2012)

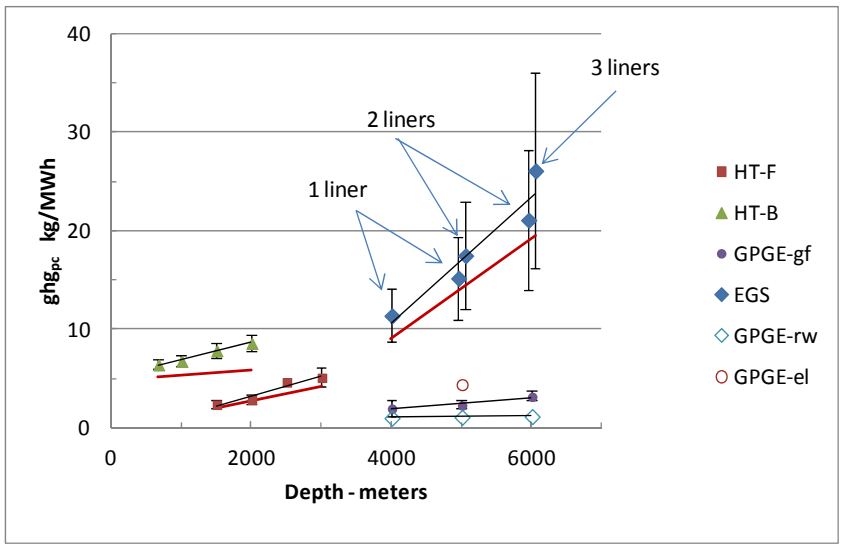

FIGURE 12 Plant Cycle GHG Emission Ratios for Several Geothermal Energy Technologies (range bars represent 1 standard deviation of combined N_{P+I} and confirmation drilling variation, red lines denote P+I wells only, with exploration not included) (Source: Sullivan et al. 2012)

The standard deviations shown in Figures 11 and 12 are the sums of the two variations just discussed; namely, those for the number of production and injection wells required to meet plant targeted capacity and those for exploration well drilling. From the lowest to highest well depths, the magnitudes of the ranges are 24–38% for EGS-B, 16–21% for HT-F, and 7–10% for HT-B. Because the quantities plotted in Figures 11 and 12 depend on both a fixed term and a well-depth-dependent variable term, the plots demonstrate a decreasing percentage of variation with decreasing well depth. This is due to energy and emissions for the plant and plant-to-well piping acting as fixed terms thus increasing their relative contribution to the total as well depths decrease.

The solid red lines in Figure 12 are trend lines representing ghg_{pc} for our geothermal scenarios without exploration. As expected, they show lower values than do their exploration counterparts. More specifically, the increase of new trend lines over old trend lines ranges from least to greatest depth: 25–33% for EGS-B, 24–46% for HT-B, and a constant 23% for HT-F. Because the HT-F facility has a 50-MW capacity and more than 20 wells, its exploration stage as treated herein is a comparatively small part of the overall ghg_{pc}. In our earlier analysis (Sullivan et al. 2011), we simply assumed that exploration amounted to one additional production well due to a lack of exploration data. Those values, not shown, would fall between the trend line pairs shown in the figure for each technology.

5.5 KEY FINDINGS ON WELL FIELD EXPLORATION MODEL RESULTS

We have advanced a model to represent the life cycle burdens of geothermal well field exploration. The model only addresses drilling activities; geoscientific methods were assumed to have negligible life cycle burdens. The model shows the following:

- Relative to the entire plant cycle, exploration drilling accounts for about 12–27% of greenhouse gas emissions (ghg_{pc}), depending on the well depth and geothermal technology used.

- The relative contribution of exploration to $\mathcal{E}_{pc}$ and ghg_{pc} decreases with an increasing number of production and injection wells.

- During exploration, confirmation well drilling consumes the majority of steel and casing used and about a third of the diesel fuel employed.

- Exploration represents a comparatively small fraction of overall well field water consumption for EGS-B and HT-F plants, and about a third of the total for HT-B plants.

- When compared to operational water consumption values from the literature, plant cycle water consumption values are about one or more orders of magnitude less.

Of all the geothermal technologies addressed, the most significant use of water for well field development was for field stimulation for EGS-B plants. The exploration drilling scheme employed in our model is based on a systematic approach used by one developer, but it may not be representative of all exploration cases.

6 GHG EMISSIONS FROM CALIFORNIA GEOTHERMAL POWER PRODUCTION

GHG emissions are generated during the production of electric power from most power generating technologies. These are fuel cycle GHGs and their magnitude can vary widely, ranging from 0 g/kWh for a photovoltaic facility to more than 1,000 g/kWh for a coal-fired power plant. The renewable power technologies promise to provide a kilowatt-hour of electricity with a much smaller GHG footprint. Geothermal power is a renewable technology, and in some cases, it has operational GHG emissions. An earlier assessment of geothermal GHG emissions for California geothermal plants is provided in Sullivan et al. (2011, 2012). The analysis in this section compares those results with current higher-quality data derived from a new regulation.

6.1 GEOTHERMAL GHG EMISSIONS BACKGROUND

GHG emissions arise when the geofluids of geothermal power plants get exposed to the atmosphere. It is widely acknowledged (Bloomfield et al. 2003; DiPippo 1999; Blaydes 1994] that due to their closed-loop nature, HT-B plants have no GHG emissions; their geofluids are returned to the reservoirs without ever getting exposed to the atmosphere. Other advantages of closed-loop systems (Blaydes 1994) include better reservoir management, very little to virtually no land subsidence, and no need for H_2S abatement equipment. Further, because the air cooling systems used at HT-B plants require no cooling water, the biocides and anti-scaling agents associated with water cooling are not needed. On the other hand, because the geofluids of hydrothermal flash and dry steam (HT-F) plants do get exposed to the atmosphere, those facilities have at least some GHG emissions, ranging from just a few grams per kilowatt-hour to values that are comparable to, or even greater than, those emitted from a NGCC power plant, (i.e., about 502 g/kWh at the plant gate) (GREET1 2012). Hence, given the operational practices of HT-F plants, the discussion that follows pertains solely to HT-F technologies and their associated fuel-use-related GHG emissions (ghg_{fu}).

Bloomfield et al. (2003) reports a weighted average emission rate of 91 g/kWh for CO_2 from U.S. geothermal power plants. When the other GHG emission (CH_4) cited in their report is considered, the total GHG emission rate becomes 110 g/kWh. Further, because the capacity weighted average included zero emissions from binary (HT-B) plants, another adjustment is required so that the average represents solely HT-F facilities. Adjusting the average to extract the 14% binary capacity surveyed, the new average GHG emission rate becomes 127 g/kWh (105 g/kWh for CO_2 only). Unfortunately, the range and distribution of U.S. geothermal emission rates were not included in that report. Its results are based on a study whose individual sources and values for provided emission rates, by agreement with geothermal plant operators, remain confidential.

A comprehensive global survey of CO_2 emissions from geothermal power plants was conducted by Bertani and Thain (2001). Other GHGs were not included in their study. The report presents range, distribution, and weighted average CO_2 ghg_{fu} results from geothermal power plants around the globe. Its ghg_{fu} data, which range from 4 to 740 g/kWh, were obtained from 85 HT-F plants, representing 85% of global capacity. Specifically, the report shows six plants

with emission rates of more than 500 g/kWh. Unfortunately, plant identities and regional locations are not given in Bertani and Thain (2001). The weighted average for the global distribution is 122 g/kWh. A similar range of CO_2 emissions (30 to 570 g/kWh, with an average of 80 g/kWh) has also been reported for plants operating in New Zealand (Rule et al. 2009), but, unfortunately, once again, the distribution of ghg_{fu} data were not reported. Although the global average ghg_{fu} data from Bertani and Thain (2001) are comparable to our adjusted weighted average from the Bloomfield et al. (2003) data (i.e., 105 g/kWh for CO_2 only), some of the global geothermal plants had ghg_{fu} values considerably greater than those from a NGCC power plant (502 g/kWh from GREET1 [2012]) operating at 47% efficiency. The question at hand is whether this is also the case for any of the HT-F plants operating in the United States.

The only publicly available information on GHG distributions from U.S. geothermal plants is provided by the California Environmental Protection Agency's (CEPA's) California Air Resources Board (CARB). Other states with geothermal facilities neither require nor routinely collect GHG emissions from such plants within their jurisdictions. However, there were a number of limitations in the California GHG emissions data used in our previous reports (Sullivan et al. 2011, 2012, 2013; Sullivan and Wang 2013), including the following: (1) not all plants reported their emissions (due to a 2,500-mt threshold level), (2) not all plants reported both CO_2 and CH_4 emissions, and (3) an unknown number of plants used a "one size fits all" emission factor as a basis for their reports. Fortunately, the new regulation requires that both CO_2 and CH_4 be reported and that only measured GHG emission values using site specific emission factors are acceptable.

In light of recent changes to the California GHG reporting regulations, the purpose of this section is to present an updated analysis of California geothermal ghg_{fu} values and their cumulative distribution function (CDF) and to compare the new findings to previous results (Sullivan et al. 2011, 2012, 2013; Sullivan and Wang 2013). Data and their sources are included herein. Note that 2011 was the transition year for the new CEPA GHG emissions reporting regulation. Hence, some additional changes in reported emissions in California may appear in GHG data for 2012, after which no further changes due to procedural adoption should occur.

6.2 GEOTHERMAL PLANT LOCATIONS

According to the Geothermal Energy Association (GEA 2012), of the 74 operating geothermal power plants in the United States, 48 are located in California. Of the 1,615 MW of geothermal running capacity in California (GEA 2012), only about 91 MW is from HT-B plants; the rest is from HT-F plants. Hence, 94% of California's geothermal power capacity is from HT-F plants. On the other hand, Nevada has 237 MW of running geothermal capacity, of which 151 MW is from binary. Hence, Nevada's geothermal running capacity from HT-F plants is only 36%. In Utah, 75% of the state's 48 MW of geothermal running capacity is from HT-F plants, the rest is from HT-B plants. There are even smaller amounts in Idaho and Hawaii. In total, the United States has 1,942 MW of capacity, of which 1,646 MW is from HT-F plants and 296 MW is from HT-B plants, resulting in California representing 93% of the nation's HT-F generation.

At this time, California is the only state that requires power plants to report GHG emissions if they are above a certain threshold (2,500 mt emitted annually). Fortunately, these data are publicly available, which permits an estimation of an emissions rate distribution function for California geothermal power plants. However, because GHG emissions from geothermal sites tend to be highly site specific (Rule et al. 2009), we cannot, with confidence, determine the corresponding U.S. distribution on the basis of the California data, Nevertheless, given that California generates 93% of the nation's HT-F power, the distribution there might be a good approximation of the U.S. distribution for nonbinary plants.

6.3 GHG EMISSIONS AND ELECTRICITY FROM CALIFORNIA GEOTHERMAL POWER PLANTS

As per Equations 1 and 2 in Section 2, fuel cycle fossil energy use and GHG emissions are generally not the only life cycle burdens associated with electric power production; plant cycle emissions are also incurred. For the reasons discussed in Section 3, we ignore O&M and dcm life cycle burdens for HT-F plants; moreover, there are no fossil energy or emissions generated during fuel (geofluid) production for those plants either. Hence, Equations 1 and 2 become:

$$\mathcal{E}_{tot} = \mathcal{E}_{fu} + \mathcal{E}_{pc} \tag{3}$$

and

$$ghg_{tot} = ghg_{fu} + ghg_{pc} \tag{4}$$

To compute ghg and $\mathcal{E}$ values for our geothermal power life cycle analysis, specific values for GHG and E_{out} are required. We obtained GHG emission values from CEPA (see URL given in CEPA [2010] for data files for 2010 and also for other years). We used all available detailed data for reporting entities, which only covers the years from 2008 to 2012. The corresponding electricity production data for those entities were extracted from the California Energy Commission's (CEC's) website (CEC 2013). Further, with each entity we associated a "running capacity" (GEA 2012) value. The running capacities were used as described here to develop an emission rate CDF. For the reader's convenience, all of these GHG and generation data are included in the Appendix, Tables A-6 to A-10.

An inspection of these data sources reveals that there are more entries for energy generation and running capacity than entries for reported GHG emissions. From a ghg_{fu} distribution point of view, this highlights a shortcoming of the CEPA data. Of the 36 operating HT-Fs in California, only 12 or 13 values are routinely reported to CEPA. For example, Geysers, operated by Calpine, has 17 operating plants (nominally 20), but it submits only one GHG value, thus averaging out any variation in emission rates among those plants. Overall, this leads to some loss in the emission rate's level of detail. Because of this aggregation in reported GHG values, we summed the listings of plant running capacities and amounts of electricity generated annually to correspond with the reporting entities listed in the CEPA data. Fortunately, there is still enough detail in the reported GHG values to estimate the CDFs and corresponding averages.

6.4 RESULTS: CALIFORNIA GHG EMISSIONS

Because of the limitations just discussed with regard to pre-2011 CEPA GHG data, we first compared 2011 and 2012 CEPA ghg_{fu} data under the new regulation for each reporting geothermal entity with its corresponding average over the regulation pre-revision years of 2008, 2009, and 2010. (These are henceforth denoted 3YA for three-year-averaged data.). The comparison is shown in Figure 13. Of the 1,524 MW of running capacity for HT-F plants in California, the data, depending on year, cover from 1,474 to 1,512 MW of running capacity, thus representing a minimum of 97% coverage of California's HT-F running capacity. As mentioned, the newly reported ghg_{fu} data must account for both CO_2 and CH_4 emissions and be based on site-specific emission factors rather than a "one size fits all" emission factor. Again, raw numerical data for the points in the figure are given in Tables A6–A10 of the appendix. For our analysis, we assumed that the running capacities listed in GEA (2012) for the covered plants remained constant over the entire time frame (2008–2012) of the available data.

A number of features in Figure 13 merit comment. Overall, the sizes of the range bars (not the standard deviations) seen in the figure demonstrate good consistency with the 3YA data for all but four of the facilities. We chose data ranges over standard deviations because, for most plants, only three and sometimes just two values were available. In fact, all facilities except Heber have range bars, but the absolute magnitudes of many of them are so low that the bars barely show up in Figure 13. Numerical values for 3YA ghg_{fu} values are given in Table A-11. The table shows that most of the plants have relative variations (1/2 range/average) of less than 10%, two have slightly more than 10%, and three have about 20% or more. The largest variations for the 3YA data shown in Figure 13 are for Navy I, Navy II, BLM E&W, Bottle Rock, and GEM 2&3. Assuming the measurements are consistent, the observed large variations suggest that an appreciable degree of natural variation in ghg_{fu} values exist at those sites. Incidentally, small range bars for reported ghg_{fu} values indicate both measurement and calculation consistency, with little apparent natural variation in field emissions. However, consistency does not necessarily imply accuracy if, in those years, a non-site-specific emission factor was used.

A comparison of 3YA, 2011, and 2012 emission rate data sets in Figure 13 reveals considerable differences in ghg_{fu} values for a number plants. It appears that relative to 3YA values and their ranges, 2011 ghg_{fu} values are higher for Navy II, BLM E&W, Ncal_1, and Ncal_2; a little lower for J J Elmore and CalEnrg 1; and about the same for the remaining six reporting entities. Cases in which the 2011 values are significantly outside the range bars of the 3YA data might be a consequence of the fact that some plants started reporting their GHG emissions as per the new reporting protocol in 2011, the transition year to the new rules. Moreover, a comparison of 2012 ghg_{fu} results with the other sets shows that GEM 2&3, Navy I, Geysers, and Bottle Rock have statistically equivalent values across the three sets; all four California Energy plants (J J Elmore, J M Leathers, Region 1, and Region 2 [labeled CalEnrg 1 and CalEnrg 2 in figure]) report markedly lower 2012 ghg_{fu} values; and four plants (Navy II, BLM E&W, Ncal_1, and Ncal_2) show both 2011 and 2012 results well above their 3YA counterparts. Clearly, for some facilities, the new California GHG reporting protocol has led to changes in reported ghg_{fu} values that make them presumably more accurate.

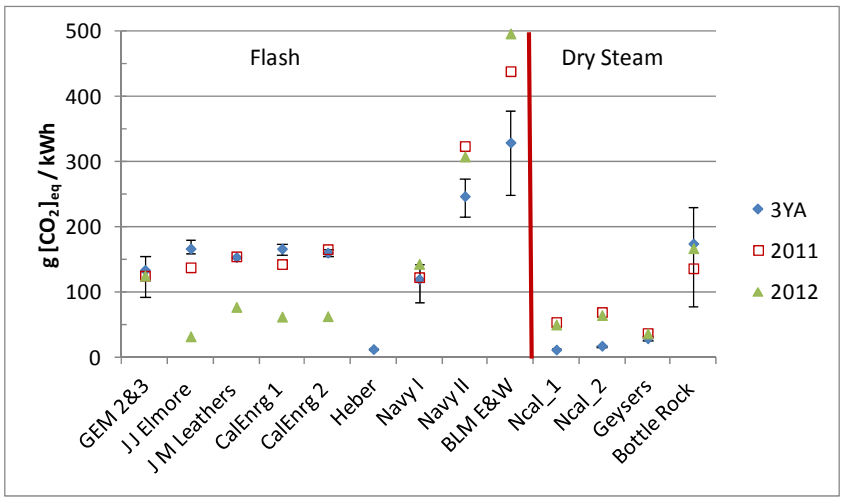

FIGURE 13 Comparison of 2008–2012 GHG Emission Rates from California HT-F Plants, Both Flash and Dry Steam (averages taken over 2008, 2009, and 2010 data; error bars represent ranges)

The precise reasons for the change in facilities' ghg_{fu} values that were different before and after the revised protocol are not known. Reduced ghg_{fu} values might be the result of using more representative emission factors (most likely) or of implementing new operational practices, such as the reinjection of unflashed brines. Higher values might be due to more complete reporting of all GHG (CO_2 and CH_4) emissions, use of more representative emission factors, or both.

TABLE 4 Average Geothermal GHG Emission Rates (g/kWh) in Various Years in California

Average	2008	2009	2010	2011	2012	3YA[a]
Running capacity weighted average	89	103	105	117	103	99
Average HT-F plant ghg_{fu} values	120	143	149	159	136	137

[a] Average of 2008, 2009, and 2010 data.

While there are significant differences between 2012, 2011 and 3YA emissions rate values for some plants, their impact on system averages are much smaller. Two types of ghg_{fu} averages appear in Table 4, capacity weighted average and the average of all California HT-F plant ghg_{fu} values. The former better represents overall GHG emissions from California HT-F plants. Although the averages given in the table represent each of the years considered, we focus on comparing 3YA with 2012 values, the latter being presumably the most current and accurate. As seen in the table, the 2012 weighted average value is only 4% higher than its corresponding 3YA value, whereas the 2012 all-plant average is, in effect, identical to its 3YA counterpart (i.e., there is a small but trivial difference, but they are statistically equivalent). But there is another trend in the table that merits comment. It appears that the 2008 values of both averages in Table

4 are appreciably lower than their 2009 and 2010 counterparts. This can be attributed to the Coso plants for two reasons: (1) they had markedly lower ghg_{fu} values in 2008 than in 2009 and 2010, and (2) those plants account for 20% of California's HT-F running capacity and 40% of California HT-F GHG emissions.

We also point out that our adjusted Bloomfield et al. (2003) weighted average (127 g/kWh) is higher than any of averages given in Table 4. The likely reason for this is that their study included HT-F plants from other states in addition to those in California.

Figure 14 displays two "fraction of total running capacity" versus emission rate CDFs: one from worldwide data (Bertani and Thain [2001]) and the other from 2012 California data. The data shown in the figure represent the cumulative fraction of running capacity versus the weighted average ghg_{fu} values for 50-g/kWh bins at the low end and for 100-g/kWh bins at the high end of the distributions. Although the two CDFs appear to be quite similar, there are differences. The global CDF seen in Figure 14 has a ghg_{fu} value higher than any California ghg_{fu} value. In fact, six plants in the global study had ghg_{fu} values higher than the ghg_{fu} for a NGCC plant (502 g/kWh), whereas only one California plant had a ghg_{fu} value (496 g/kWh) close to the NGCC value. The figure also illustrates that the California CDF is weighted more toward the lower end of the g/kWh range, which is why its overall weighted average ghg_{fu} value (103 g/kWh) is lower than the value of its global counterpart (122 g/kWh). And because the global average value accounts for CO_2 only, it could be higher yet if CH_4 emissions had been included. In fact, 85% of California's running HT-F capacity has ghg_{fu} values lower than about 170 g/kWh.

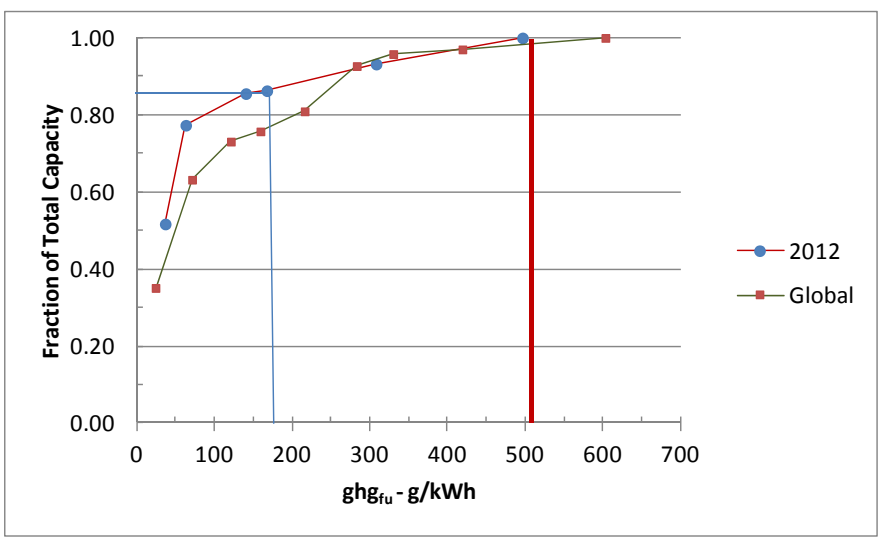

FIGURE 14 GHG Emission Rate (ghg_{fu}) Cumulative Distribution Functions for Global and 2012 California HT-F Capacities (vertical red line shows fuel cycle emissions [502 g/kWh] at the plant gate from a NGCC plant [GREET1 2012]; blue lines show that 85% of California running capacity emits less than 170 g/kWh)

Even with higher-quality GHG data at hand, the data's significance can be called somewhat into question. The sites for most flash and steam geothermal power plants are locations where the resource is manifested at the surface (e.g., as hot springs, fumaroles, mud pots, steam vents, geysers). These features demonstrate that a hot resource is present below and suggest that a background level of GHG emissions is already being naturally released at those locations. The question at hand pertains to the degree to which power plant activity affects overall (plant plus background) emissions from the area. Further questions are will the GHG emissions naturally decrease over time, and if so, by how much? Quantitative answers to these questions await results from future research.

6.5 KEY FINDINGS ON GEOTHERMAL GHG EMISSIONS

This section presents an analysis of GHG emissions from California HT-F plants, with an emphasis on the most recent data reported to CEPA. From the data, we made the following conclusions:

- Overall, 2011 and 2012 emissions data reported to CEPA show that the revised reporting regulation has resulted in changes to the distribution function for California HT-F GHG emissions. For some plants, ghg_{fu} values are lower; in others, they are higher. For a number of plants, there are no changes in values.

- Reported emissions now unambiguously represent both CO_2 and CH_4 emissions based on site-specific emission factors.

- The running capacity weighted average emissions rate for California HT-F plants is 103 g/kWh.

- In California, the running capacities for 85% of the state's HT-F plants have ghgfu values of 170 g/kWh or less; two plants had values of more than 300 g/kWh.

This page intentionally blank.

7 GEOTHERMAL VERSUS OTHER POWER GENERATING TECHNOLOGIES

The focus of this report is to complete our LCA of geothermal power production. In this section, geothermal $\mathcal{E}_{tot}$ and ghg_{tot} values are compared with those from other power generating technologies. For each power generating technology, all components of these two metrics as expressed in Equations 1 and 2 are included where significant. Results are shown in Figures 15 and 16; numerical values are provided in Table A-1. Results revealed in the two figures and the table include (1) O&M data for all covered technologies, (2) updated well field exploration data (see Section 5) added to the geothermal plant cycle metrics, and (3) updated operational GHG emission data for California HT-F plants.

Figures 15 and 16 show that $\mathcal{E}_{tot}$ and ghg_{tot} values for any of the renewable technologies range from 5 to 10 times less than values from fossil-fuel-fired power plants. Figure 15 (and Table A-1) shows that ghg_{pc} values for geothermal plants can range from as low as 4 to almost 30 g/kWh. Even considering a potential increase of one-third in GHG emissions due to O&M activities, ghg_{tot} values for HT-B and EGS are at least an order of magnitude less than ghg_{tot} values for fossil-fuel-fired power. Even for HT-F plants, the ghg_{tot} values are still considerably lower than those for fossil plants, despite the fact that HT-F plants are the only geothermal plants with fuel cycle GHG emissions, which arise from fuel use (i.e., ghg_{fu}). This is covered in detail in Section 6.

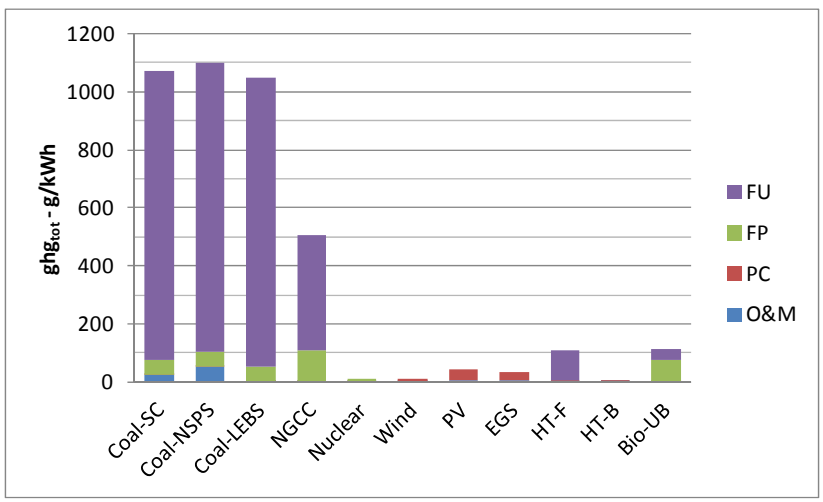

FIGURE 15 Components of Life Cycle GHG Emissions at the Plant Gate for a Range of Power Generating Technologies (including O&M; fuel use [FU] and fuel production [FP] from GREET1 [2012]; and plant cycle [PC] from Sullivan et al. [2010, 2011])

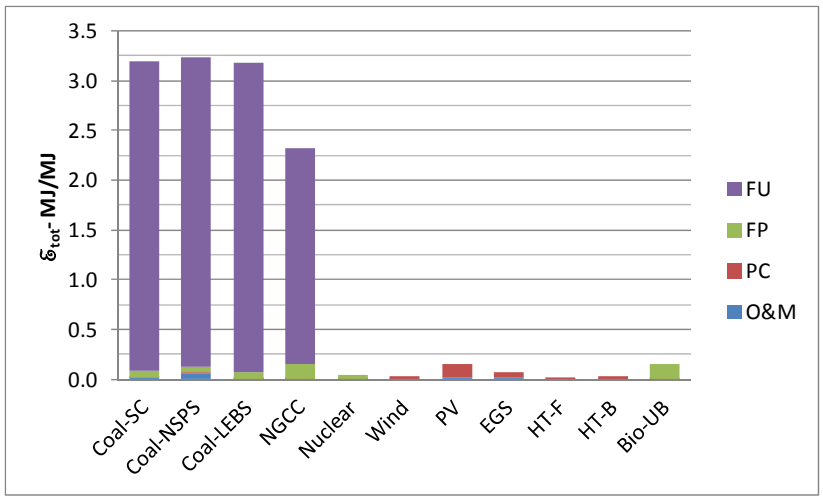

FIGURE 16 Components of the Life Cycle Energy Ratio at the Plant Gate for a Range of Power Generating Technologies (including O&M; fuel use [FU] and fuel production [FP] from GREET1 [2012]; plant cycle [PC] from Sullivan et al. [2010, 2011])

Further, except for HT-F plants, it is evident in both figures that the only apparent components of the $\mathcal{E}_{tot}$ and ghg_{tot} values for the renewable power generating technologies arise from the plant cycle stage, followed by their O&M counterparts (see Table A-1), which are considerably smaller. However, this is not the case for two coal scenarios, for which, except for the fuel cycle components, the O&M contributions are the next largest in magnitude. This is a consequence of the variable O&M burdens associated with FGD processes. Nevertheless, despite their magnitude, even the largest coal $ghg_{o\&m}$ values make only a small contribution to their "total" counterparts. On the other hand, the O&M contribution, which is not evident in the figures, is still larger than that of the plant cycle counterparts for coal and NGCC plants (see Table A-1). The former employs a regenerative sulfur capturing medium, and, for NGCC, emissions of NO_x rather than of sulfur are the emissions of importance.

A closer inspection of Figures 15 and 16 shows a curious result, in which HT-F shows no fossil fuel consumption in Figure 16 yet shows fossil carbon emissions in Figure 15. This circumstance is discussed in Sullivan et al. (2010, 2011, 2012) and also, in considerable detail, in Section 6. Briefly, the reason for this is that the geofluid used in HT-F plants gets exposed to the atmosphere after it has passed through the turbine, thus releasing dissolved CO_2 and CH_4. However, no fossil fuels have been consumed. The value shown for ghg_{fu} in Figure 15 is the running capacity weighted average for California HT-F plants based on 2012 data.

Nuclear and renewable power technologies do not consume fossil fuels to produce electricity. The only life cycle phase apparent for nuclear plants in Figures 15 and 16 is the fuel production stage, which employs fossil fuels to mine and enrich uranium fuel rods. The sum of the plant cycle and O&M energy and emissions ratios for nuclear power production is about one-twentieth (see Table A-1) of the corresponding $\mathcal{E}_{fp}$ and ghg_{fp} values, thus demonstrating the

relative insignificance of each of the components. For the O&M stage, this conclusion echoes one shown in Warner and Heath (2012).

Also included in Figure 15 and 16 are results for another renewable power technology: biomass-fired utility boiler (Bio-UB) plant. Despite its status as a renewable technology, Bio-UB has both fuel use and fuel production GHG emissions and consumes fossil energy for fuel production. Its finite $\mathcal{E}_{fp}$ value is incurred during the harvesting and transport of power plant fuel (forestry residues), processes that require fossil fuel from which ghg_{fp} emissions arise. Even though there are no fossil fuels being burned during fuel use, GHGs (N_2O and CH_4) emissions arise due to incomplete combustion in the boiler, thus generating fuel use emissions (ghg_{fu}). The magnitude of ghg_{tot} from a Bio-UB plant is comparable to that from an average HT-F plant.

Finally, geothermal power plants offer significant benefits with regard to reductions in both GHG emissions and fossil fuel use when compared with fossil power plants. In addition, geothermal plants, when sited over commercially viable resources, offer trouble-free baseload electric power production virtually full time (at a 95% capacity factor).

This page intentionally blank.

8 CONCLUSIONS

This report addresses a series of topics and completes the LCA of geothermal and other electric power production technologies. It includes an analysis of the O&M and decommissioning stages of power production, an assessment of 10 new geothermal scenarios, an updated model of geothermal well field exploration, an assessment of operational GHG emissions from geothermal HT-F plants in California, and, finally, a comparison of geothermal power-generating technologies with other power-generating technologies. These results complement a series of earlier reports by Argonne National Laboratory (Sullivan et al. 2010, 2011, 2012, 2013). A summary of results developed herein follows:

- The magnitude of the O&M and decommissioning stages of the power plant life cycle were quantified.
    - GHG emissions associated with the O&M component of the power plant infrastructure stage ($ghg_{o\&m}/ghg_{inf}$) range widely, from almost zero for wind power plants to more than 95% for coal power plants.
    - For geothermal plants, $\mathcal{E}_{o\&m}/\mathcal{E}_{inf}$ and $ghg_{o\&m}/ghg_{inf}$ depend on well depth, with magnitudes of about 20% for EGS plants (6-km wells), 12% for HT-B plants (1-km wells), and 28% for HT-F plants (2.5-km wells). The O&M contribution with regard to geothermal plants is mostly due to well replacement.
    - The largest $ghg_{o\&m}$ value among all of the technologies covered is that for coal plants; it represents more than 95% of its ghg_{inf}. This is due to very large variable O&M burdens associated with FGD relative to the small ghg_{pc} value for coal plants.
    - The decommissioning stage is negligible.
- Ten new geothermal scenarios, each composed of a reference case and an improved case, were advanced by the LCOE group to explore the impacts of well depth, resource temperature, plant lifetime, plant capacity, geofluid flow rates, and type of technology on costs and environmental performance.
    - Scenarios covered EGS-B, EGS-F, HT-B, and HT-F technologies.
    - For all 10 scenario pairs, the improved cases had lower LCOE (¢/kWh), $\mathcal{E}_{tot}$, and ghg_{tot} values than the associated reference cases.
    - These reductions were greater for EGS scenarios, primarily due to the 20-year plant lifetimes assumed for reference cases versus the 30-year lifetimes assumed for improved cases.
    - Also, however, decreases in "improved case" LCOE, $\mathcal{E}_{tot}$, and ghg_{tot} values from those for their reference counterparts are due to decreases in the amounts of well field

materials and drilling fuels per megawatt of plant capacity, which, in turn, depend on the number and depths of wells.

- Our exploration model permitted revised estimates of $\mathcal{E}_{tot}$ and ghg_{tot} values for geothermal power systems.
    - The model is based on published data and has been reviewed by industry. It accounts for core hole, slim hole, and confirmation well drilling. A drilling success rate is also included.
    - Overall, the new $\mathcal{E}_{tot}$ and ghg_{tot} values fell into the range defined in our earlier work.
    - Because exploration GHG emissions are assumed to be independent of plant size, the exploration component of ghg_{pc} (g/kWh) decreases with increasing plant capacity.
    - The exploration component of ghg_{pc} ranges from about 20% for large plants with multiple wells to as much as 32% for small plants with few wells.
- GHGs emitted during operations of HT-F (flash and dry steam) plants arise when geofluids are exposed to the atmosphere. We reviewed several years of data on the subject and found the following:
    - For California, ghg_{fu} values for 2012 ranged from 32 to 496 g/kWh, with a capacity-weighted average of 103 g/kWh.
    - Of all California HT-F plants running at capacity, 85% emit 170 g/kWh (32% of those emitted from an NGCC plant) or less of operational GHGs.
    - Less than 10% of HT-F plants globally have emission rates that exceed the rate of 502 g/kWh from an NGCC plant. California has only one plant that emits about that amount.
    - With regard to reporting geothermal entities in California, a comparison of the 2011 and 2012 data (gathered under a revised emission reporting protocol) with data from previous years shows an increase in reported emissions for four plants, a substantial decrease for four plants, and a statistically equivalent amount for four plants.
- Finally, when ghg_{tot} values for the geothermal technologies studied herein were compared with those of their fossil counterparts, EGS-B and HT-B technologies were found to have values that were lower by at least one order of magnitude.

Of the renewable technologies, geothermal electric power offers a clear carbon reduction benefit over its fossil counterparts.

9 REFERENCES

Augustine, 0C., and K.R. Young, 2010, *Updated U.S. Geothermal Supply Curve,* NREL/CP-6A2-47458, presented at Stanford Geothermal Workshop, Stanford, Calif., Feb. 1.

Benoit, D., J. Moore, and C. Goranson, 2005, "Core Hole Testing and Drilling at the Lake City, California Geothermal Field," in Proceedings of the Geothermal Resources Council (GRC) Annual Meeting 2005, Reno, Nev., Sept. 25–28, *GRC Transactions,* Vol. 29.

Beerten, J., E. Laes, G. Meskens, and W. D'haeseleer, 2009, "Greenhouse Gas Emissions in the Nuclear Life Cycle: A Balanced Appraisal," *Energy Policy* 37:5056–5068.

Bertani, R., and I. Thain, 2001, "Geothermal Power Generating Plant CO_2 Emission Survey," Rev. 1.0, International Geothermal Association, Oct., http://www.jeotermaldernegi.org.tr/ian%20i.htm, accessed Aug. 2010.

Blaydes, P.E., 1994, "Environmental Advantages of Binary Power Plants Can Enhance Development Opportunities," *Geothermal Resources Council Transactions* 18:121–125.

Bloomfield, K.K., J.N. Moore, and R.M. Neilson, Jr., 2003, "Geothermal Energy Reduces Greenhouse Gases," *Climate Change Research*, pp. 77–79, March/April.

CEC (California Energy Commission), 2013, *QFER CEC-1304 Power Plant Owner Reporting Database,* "Annual Generation-Plant Unit.php" or "Source Files," http://www.energyalmanac.ca.gov/electricity/web_qfer/, accessed May 13, 2013.

CEPA (California Environmental Protection Agency), 2010, "Air Resources Board, Reported Emissions, Facility Emissions," http://www.arb.ca.gov/cc/reporting/ghg-rep/ghg-rep.htm, accessed Aug. 16, 2011.

Clark, C.E., C.B. Harto, J.L. Sullivan, and M.Q. Wang, 2010, *Water Use in the Development and Operation of Geothermal Power Plants,* ANL/EVS/R-10/5, Argonne National Laboratory, Argonne, Ill.

Clark, C.E., C.B. Harto, and W.A. Troppe, 2011, *Water Resource Assessment of Geothermal Resources and Water Use in Geopressured Resources,* ANL/EVS/R-11/10, Argonne National Laboratory, Argonne, Ill.

Clark, C.E., C.B. Harto, J.R, Schroeder, L.E. Martino, and R.M. Horner, 2012, *Life Cycle Water Consumption and Water Resource Assessment for Utility Scale Geothermal Systems: An In-Depth Analysis of Historical and Forthcoming EGS Projects,* ANL/EVS/R-12/8, Argonne National Laboratory, Argonne, Ill.

DiPippo, R., 1999, "Small Geothermal Power Plants: Design, Performance, and Economics," *GRC Bulletin,* June, pp. 1–8.

DOE (U.S. Department of Energy), 2010, *A History of Geothermal Energy Research and Development in the United States, 1976–2006, Volume 3: Reservoir Engineering,* http://www1.eere.energy.gov/geothermal/pdfs/zgeothermal_history_3_engineering.pdf, accessed March 16, 2011.

EIA (Energy Information Administration), 2010a, *Annual Energy Outlook 2010*, Tables A8 and A16, U.S. Department of Energy, http://www.eia.doe.gov/oiaf/aeo/index.html.

EIA, 2010b, *Updated Capital Cost Estimates for Electricity Generation Plants,* http://www.eia.gov/oiaf/beck_plantcosts/pdf/updatedplantcosts.pdf.

EPRI (Electric Power Research Institute), 1994, *Next Generation. Geothermal Power Plants,* Report RP 3657-01, Tables 4-1 and 4-2.

Frankl, P., E. Menichetti, M. Raugei, S. Lombardelli, and G. Prennushi, 2006, *Final Report on Technical Data, Costs and Life Cycle Inventories of PV Applications,* Deliverable 11.2-RS Ia for Project No. 502687, New Energy Externalities Developments for Sustainability (NEEDS) Integrated Project, Rome, Italy.

Fthenakis, V.M., and H.C. Kim, 2007, "Greenhouse-Gas Emissions from Solar Electric- and Nuclear Power: A Life-Cycle Study," *Energy Policy* 35(4):2549–2557.

GEA (Geothermal Energy Association), 2012, "Geothermal Plants," http://geo-energy.org/plants.aspx, accessed Oct. 17, /2012.

GETEM (Geothermal Electricity Technology Evaluation Model), 2013, "Geothermal Electricity Technology Evaluation Model," http://www1.eere.energy.gov/geothermal/getem.html, last accessed Sept. 5, 2013.

GREET1, 2012, "Greenhouse Gases, Regulated Emissions and Energy in Transportation (GREET) Model," http://greet.es.anl.gov/greet_1_series, accessed July 31, 2012.

Hsu, D.D., P. O'Donoughue, V. Fthenakis, G.A. Heath, H. Chul, C.H. Kim, P. Sawyer, J. Choi, and D.E. Turney, 2012, "Life Cycle Greenhouse Gas Emissions of Crystalline Silicon Photovoltaic Electricity Generation: Systematic Review and Harmonization," *J. Industrl. Ecol.* 16(S1):S122–S135.

ISO (International Standards Organization), 1997, "Environmental Management — Life Cycle Assessment — Principles and Framework," International Standard ISO/FDIS 14040.

ISO, 1998, "Environmental Management — Life Cycle Assessment — Goal and Scope Definition and Inventory Analysis," International Standard ISO 14041.

ISO, 2000, "Environmental Management — Life Cycle Assessment — Life Cycle Impact Assessment," International Standard ISO 14042.

Jennejohn, D., 2009, *Research and Development in Geothermal Exploration and Drilling,* Geothermal Energy Association, Washington, D.C.

Koomey, J., and N.E. Hultman, 2007, "A Reactor-Level Analysis of Busbar Costs for U.S. Nuclear Plants 1970–2005," *Energy Policy* 35:5630–5642.

Lave, L.B., E. Cobas-Flores, C.T. Hendrickson, and F.C. McMichael, 1995, "Using Input-Output Analysis to Estimate Economy-wide Discharges," *Environmental Science & Technology* 29: 420–426.

Mason, J.M., V.M. Fthenakis, T. Hansen, and H.C. Kim, 2006, "Energy Pay-Back and Life Cycle CO_2 Emissions of the BOS in an Optimized 3.5 MW PV Installation," *Progress in Photovoltaics Research and Applications* 14:179–190.

McNerney, J., J.D. Farmer, J.E.Trancik, 2011, "Historical Costs of Coal-Fired Electricity and Implications for the Future," *Energy Policy* 39:3042–3054.

OpenEI, 2012, *Geothermal Energy,* choose topic of "Exploration," http://en.openei.org/wiki/Gateway:Geothermal, accessed April 23, 2012.

Rotty, R.M., A.M. Perry, and D.B. Reister, 1975, *Net Energy from Nuclear Power,* IEA-75-3, Institute for Energy Analysis, Oak Ridge Associated Universities.

Rule, B.M., Z.J. Worth, and C.A. Boyle, 2009, "Comparison of Life Cycle Carbon Dioxide Emissions and Embodied Energy in Four Renewable Electricity Generation Technologies in New Zealand," *Environmental Science & Technology* 43:6406–6413.

Sanyal, S.K., and J.W. Morrow, 2011, "An Investigation of Drilling Success in Geothermal Exploration, Development and Operation," *GRC Transactions* 35:233–237.

Sargent and Lundy, 2009, New Coal-Fired Power Plant Performance and Cost Estimates, SL-009808, Chicago, Ill., Aug. 28, http://www.docstoc.com/docs/46323793/New-Coal-Fired-Power-Plant-Performance-and-Cost-Estimates.

Shevenell, L., 2012a, "The Estimated Costs as a Function of Depth of Geothermal Development Wells Drilled in Nevada," *GRC Transactions* 28:121–128.

Shevenell, L., 2012b, "The Rate of Success of Well Drilling in Nevada," *GRC Transactions* 28:129–139.

Spath, P.L., and M.K. Mann, 2000, "Life Cycle Assessment of a Natural Gas Combined-Cycle Power Generation System," NREL/TP-570-27715, National Renewable Energy Laboratory, Golden, Colo.

Spath, P.L., M.K. Mann, and D.R. Kerr, 1999, "Life Cycle Assessment of Coal-Fired Power Production," NREL/TP-520-25119, National Renewable Energy Laboratory, Golden, Colo.

Sullivan, J.L., C.E. Clark, J. Han, and M. Wang, 2010, *Life-Cycle Analysis Results of Geothermal Systems in Comparison to Other Power Systems,* ANL/ESD/10-5, Argonne National Laboratory, Argonne, Ill.

Sullivan, J.L., C.E. Clark, L. Yuan, J. Han, and M. Wang, 2011, *Life-Cycle Analysis Results of Geothermal Systems in Comparison to Other Power Systems*, *Part II,* ANL/ESD/11-12, Argonne National Laboratory, Argonne, Ill.

Sullivan, J.L., E. Frank, J. Han, A. Elgowainy, and M.Q. Wang, 2012, *Geothermal Life-Cycle Assessment – Part 3,* ANL/ESD/12-15, Argonne National Laboratory, Argonne, Ill.

Sullivan, J.L., C. Clark, J. Han, C. Harto, and M. Wang, 2013, "Cumulative Energy, Emissions, and Water Consumption for Geothermal Electric Power Production," *J. Renewable & Sustainable Energy* 5, 023127.

Sullivan, J.L., and M.Q. Wang, 2013, "Life Cycle Greenhouse Gas Emissions from Geothermal Electricity Production," *J. Renewable & Sustainable Energy* 5, 063122, 1–13.

Tsoulfanidis, N., 1981, "Energy Analysis of Coal, Fission, and Fusion Power Plants," *Nuclear Technology Fusion* 1:238–254.

Vattenfall (Vattenfall AB Nuclear Power), 2010, *Certified Environmental Product Declaration EPD® of Electricity from Forsmark Nuclear Power Plant,* S-P 00021 2013-12-13 and S-P 00026 2010-12-16, UNCPC Code 17, Group 171–Electrical Energy, http://www.environdec.com/Detail/?Epd=5991#.UgFAIm2neyE, accessed Aug. 6, 2013.

Vestas (Vestas Wind Systems A/S), 2006, "Life Cycle Assessment of Electricity Delivered from an Onshore Power Plant Based on Vestas V82-1.65 MW Turbines," Dec. 29, http://www.vestas.com/, accessed Aug. 2010.

Warner, E.S., and G.A. Heath, 2012, "Life Cycle GHG Emissions of Nuclear Power Electricity Generation: Systematic Review and Harmonization," *Journal of Industrial Ecology* 16:S73–S9, supplemental material.

White, S.W., and G.L. Kulcinski, 1998, *Birth to Death Analysis of the Energy Payback Ratio and CO_2 Gas Emission Rates from Coal, Fission, Wind and DT Fusion Electrical Power Plants,* UWFDM-1063, Fusion Technology Institute, Wisc.

APPENDIX A: SUPPORTING MATERIAL

TABLE A-1 Modeling Details and Corresponding Energy and GHG Ratio Values for a Series of Power Production Technologies by Life Cycle Stage

Technology	Coal			NGCC	Nuclear	Wind	PV	EGS-B	HT-F	HT-B
Scenario[a]	1	2	3	4	5	6	7	8	9	10
% MPR replaced	10[b]	10[b]	10[b]	10[b]	10[b]	10[b]	10[c]	GT[d]	GT	GT
% wells replaced	NA[e]	NA	NA	NA	NA	NA	NA	50[f]	50[f]	50[f]
Well depth (km)	NA	NA	NA	NA	NA	NA	NA	6	2.5	1
Energy ratio per stage[g] (MJ/MJ)										
$\mathcal{E}_{pc}$	0.002	0.002	0.002	0.001	0.0014	0.025	0.13	0.057	0.0112	0.022
$\mathcal{E}_{o\&m}$	0.021	0.063	0.004	0.002	0.0009	0.0016	0.017	0.019	0.004	0.002
$\mathcal{E}_{fp}$	0.063	0.063	0.063	0.190	0.037	0.000	0.000	0.000	0.000	0.000
$\mathcal{E}_{fu}$	3.10	3.10	3.10	2.07	0.000	0.000	0.000	0.000	0.000	0.000
$\mathcal{E}_{tot}$	3.20	3.24	3.18	2.32	0.039	0.030	0.156	0.076	0.016	0.024
GHG ratio per stage[g] (g/kWh)										
ghg_{pc}	0.7	0.831	0.831	0.34	0.59	8.9	35.8	27.7	4.1	5.7
$ghg_{o\&m}$	22.8	51.4	0.84	0.32	0.23	0.16	4.43	6.89	1.51	0.72
ghg_{fp}	56.4	56.4	56.4	117	9.90	0.0	0.0	0.0	0.0	0.0
ghg_{fu}	1064.	1064.	1064.	419	0.0	0.0	0.0	0.0	103	0.0
ghg_{tot}	1070.	1099.	1048.	504	10.7	9.1	42.2	34.6	109	6.4

[a] Source of information per scenario (i.e., column) number:
- 1 Sargent and Lundy (2009)
- 2 NSPS (New Source Performance Standard) plant = Spath et al. (1999)
- 3 Low emission boiler system = Spath et al. (1999)
- 4 Spath and Mann (2000)
- 5 Vattenfall (2010)
- 6 Sullivan et al. (2010), assuming replacement of half of the gearbox
- 7 Sullivan et al. (2011), assuming 10% steel, aluminum, and silicon replacement rate
- 8–10 Sullivan et al. (2011)

[b] Steel.

[c] Steel, aluminum, and silicon.

[d] GT = For geothermal replacement done at wells, see row below (% wells replaced).

[e] NA = not applicable.

[f] Steel, and cement for wells.

[g] Life-cycle stages: pc = plant cycle, o&m = operations and maintenance, fp = fuel production, fu = fuel use; tot = their sum (shaded rows). Data for fp and fu stages taken from GREET1 (2012).

TABLE A-2 GETEM Input for Alternative Enhanced Geothermal System Plant Scenario Pairs: Reference Cases (a) and Improved Cases (b)[a]

Item	Scenario									
Resource/technology ID	1a	1b	2a	2b	3a	3b	4a	4b	5a	5b
Technology description	Ref	Imprvd	Ref	Imprvd	Ref	Imprvd	Ref	Imprvd	Ref	Imprvd
Technology year	2012	2030	2012	2030	2012	2030	2012	2030	2012	2030
LCOE (¢/kWh)	77.5	20.2	28.6	7.0	24.8	5.8	17.9	5.2	13.9	3.9
Power sales (MW)	10	25	15	35	20	40	25	50	30	50
Capacity factor	95%	95%	95%	95%	95%	95%	95%	95%	95%	95%
Generator type	Binary	Binary	Binary	Binary	Binary	Binary	Flash	Flash	Flash	Flash
Type of cooling	Air	Air	Air	Air	Air	Air	Wet	Wet	Wet	Wet
Temperature (°C)	100	100	150	150	175	175	250	250	325	325
Thermal drawdown (%/yr)	0.5	0.3	0.5	0.3	0.5	0.3	0.5	0.3	0.5	0.3
No. of production (P) wells required	21.5	22.7	7.6	9.4	7.9	7.8	6.4	5.7	4.2	3.2
Ratio of injection (I) wells to P wells	0.5	0.5	0.5	0.5	0.5	0.5	0.5	0.5	0.5	0.5
No. of confirmation (C) wells drilled	3.75	2	3.75	2	3.75	2	3.75	2	3.75	2
No. of successful confirmation wells	3	2	3	2	3	2	2	2	2	2
No. of successful P wells	18.5	20.7	4.6	7.4	4.9	5.8	3.4	3.7	1.2	1.2
Total no. of wells drilled (C, P, I, dry)	32.95	34.1	12.15	14.1	12.55	11.7	10.35	8.6	7.05	4.8
No. of exploration well sites	2	1.5	2	1.5	2	1.5	2	1.5	2	1.5
Well depth (km)	2	2	2.5	2.5	3	3	3.5	3.5	4	4
P well flow rate (kg/s)	40	100	40	100	40	100	40	80	40	80
Pump depth (m) for P well	78.4	114.7	44.7	87.6	18	71.6	0	0	0	0
Distance between wells (m)	1,000	NS[b]	1,000	NS	1,000	NS	1,000	NS	1,000	NS
Location of plant relative to wells	Central	Central	Central	Central	Central	Central	Central	Central	Central	Central
U.S. geographic location	SW	SW	SW	SW	SW	SW	SW	SW	SW	SW
Plant lifetime (yr)	20	30	20	30	20	30	20	30	20	30
No. of wells stimulated	9.7	10.7	2.8	4	2.9	3.2	2.2	2.2	1.1	0.9

[a] All plants are single turbine plants with well fields stimulated; assumption is no dry holes during exploration. Binary cases are in shaded columns.

[b] NS = Not specified in GETEM output, but assumed to be the same as for the corresponding reference case.

TABLE A-3 GETEM Input for Alternative Hydrothermal Plant Scenario Pairs: Reference Cases (a) and Improved Cases (b)[a]

Item	Scenario									
Resource/technology ID	6a	6b	7a	7b	8a	8b	9a	9b	10a	10b
Technology description	Ref	Imprvd	Ref	Imprvd	Ref	Imprvd	Ref	Imprvd	Ref	Imprvd
Technology year	2012	2020	2012	2020	2012	2020	2012	2020	2012	2020
LCOE (¢/kWh)	24.2	10.7	13.7	6.5	32.5	13.8	13.9	6.7	11.5	5.4
Power sales (MW)	15	25	30	50	15	25	30	50	40	50
Capacity factor	95%	95%	95%	95%	95%	95%	95%	95%	95%	95%
No. of turbines	Single	Single	Single	Single	Single	Single	Single	Single	Single	Single
Generator type	Binary	Binary	Binary	Binary	Binary	Binary	Flash	Flash	Flash	Flash
Type of cooling	Air	Air	Air	Air	Air	Air	Wet	Wet	Wet	Wet
Temperature (°C)	140	140	175	175	140	140	175	175	225	225
Thermal drawdown (%/yr)	0.4	0.4	0.4	0.4	0.4	0.4	0.5	0.5	0.5	0.5
No. of production (P) wells required	4.7	8.6	6.1	10.8	4.2	7.7	9.2	14.7	6.1	7.4
Ratio of injection (I) wells to P wells	0.75	0.75	0.75	0.75	0.75	0.75	0.75	0.75	0.75	0.75
No. of confirmation wells drilled	7	3.67	7	3.67	7	3.67	7	3.67	7	3.67
No. of successful confirmation wells	3	2	3	2	3	2	3	2	3	2
No. of successful P wells	1.7	6.6	3.14	8.79	1.2	5.7	6.2	12.7	3.1	5.4
No. of dry holes	1.0	2.0	1.55	2.53	0.9	1.7	2.6	3.6	1.5	1.6
Total no. of wells drilled (C, P, I, dry)	13.3	18.7	16.3	23.1	12.3	16.8	22.7	30.9	16.2	16.2
No. of exploration well sites	5	3	5	3	5	3	5	3	5	3
Well depth (km)	1.5	1.5	1.5	1.5	2.5	2.5	1.5	1.5	2.5	2.5
P well flow rate (kg/s)	100	100	100	100	100	100	80	80	80	80
Pump depth (m) for P wells	239.4	239.4	273.8	273.8	255	255	0	0	0	0
Distance between wells (m)	1,000	NS[b]	1,000	NS	1,000	NS	1,000	NS	1,000	NS
Location of plant relative to wells	Central	Central	Central	Central	Central	Central	Central	Central	Central	Central
U.S. geographic location	SW	SW	SW	SW	SW	SW	SW	SW	SW	SW
Plant lifetime (yr)	30	30	30	30	30	30	30	30	30	30

[a] Binary cases are in shaded columns.

[b] NS = Not specified in GETEM output, but assumed to be the same as for the corresponding reference case.

TABLE A-4 GHG Emission and Energy Ratios for the New Geothermal Power Plant Scenarios Given in Tables A-2 and A-3: Reference Cases (a) and Improved Cases (b)[a]

Scenario	System	Net Capacity (MW)	Lifetime (years)	Depth (d) (km)	No. of Wells (N)	Nd/MW (km/MW)	$\mathcal{E}_{pc}$ (kWh/kWh)	ghg_{pc} (g/kWh)	LCOE (¢/kWh)
1a	EGS-B	10	20	2	33	6.60	0.093	27.80	77.5
1b	EGS-B	25	30	2	34.1	2.73	0.036	10.34	20.2
2a	EGS-B	15	20	2.5	12.2	2.03	0.053	16.40	28.6
2b	EGS-B	35	30	2.5	14	1.00	0.026	7.70	7.02
3a	EGS-B	20	20	3	12.6	1.89	0.051	15.50	24.8
3b	EGS-B	40	30	3	11.7	0.88	0.025	7.24	5.85
4a	EGS-F	25	20	3.5	10.4	1.46	0.024	8.01	17.9
4b	EGS-F	50	30	3.5	8.6	0.60	0.008	2.62	5.15
5a	EGS-F	30	20	4	7.1	0.95	0.017	5.71	13.9
5b	EGS-F	50	30	4	4.8	0.38	0.006	1.96	3.91
6a	HT-B	15	30	1.5	13.3	1.33	0.025	7.19	24.2
6b	HT-B	25	30	1.5	18.7	1.12	0.024	6.77	10.7
7a	HT-B	30	30	1.5	16.3	0.82	0.022	6.16	13.7
7b	HT-B	50	30	1.5	23.1	0.69	0.021	5.91	6.5
8a	HT-B	15	30	2.5	12.3	2.05	0.034	10.59	32.5
8b	HT-B	25	30	2.5	16.8	1.68	0.031	9.49	13.8
9a	HT-F	30	30	1.5	22.7	1.14	0.009	2.99	13.9
9b	HT-F	50	30	1.5	30.9	0.93	0.008	2.57	6.7
10a	HT-F	40	30	2.5	16.2	1.01	0.010	3.70	11.5
10b	HT-F	50	30	2.5	16.2	0.81	0.009	3.10	5.5

[a] Shaded rows highlight short-lifetime (20-year) scenarios.

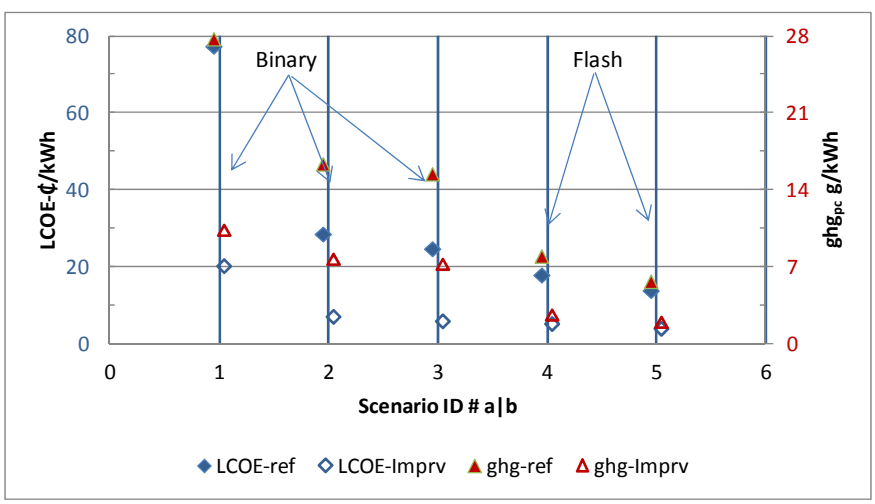

FIGURE A-1 EGS Binary and Flash Scenario LCOE and Plant Cycle GHG Emissions (g/kWh): Reference Cases (a) Versus Improved Cases (b)

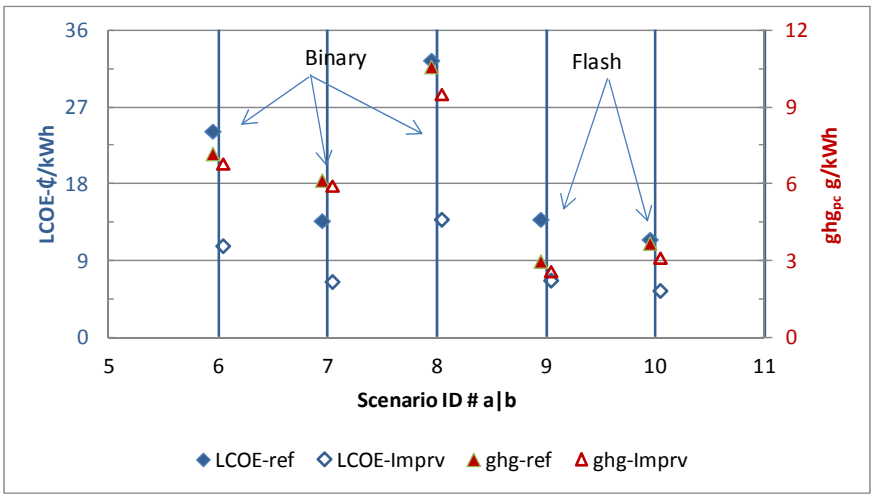

FIGURE A-2 Hydrothermal Binary and Flash Plant LCOE and Plant Cycle GHG Emissions (g/kWh): Reference Cases (a) Versus Improved Cases (b)

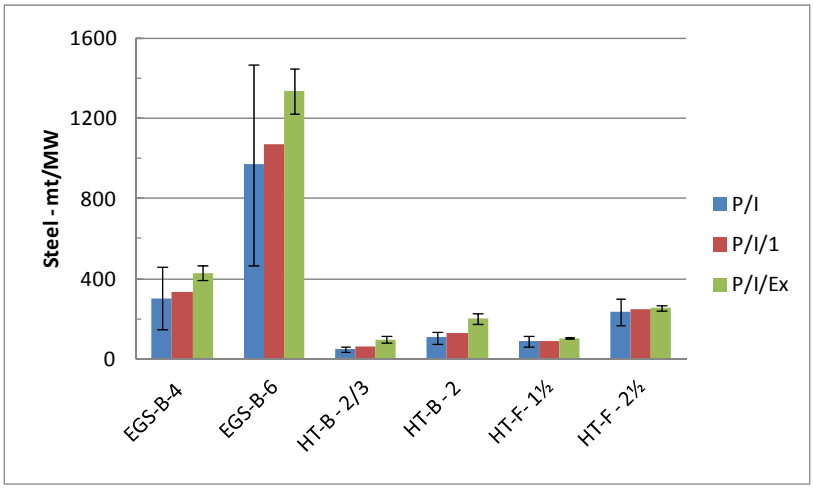

FIGURE A-3 Steel Material-to-Power Ratios (mt/MW) for the Indicated Geothermal Technologies (postscript numbers indicate well depths [km]; error bars are ±1 standard deviation, representing well number variation for P/I , failed confirmation well variation for P/I/Ex; P_1 = 0.6)

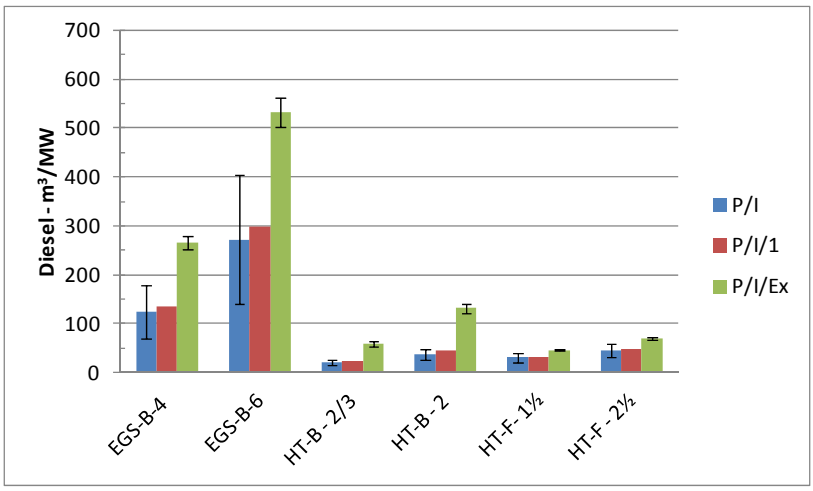

FIGURE A-4 Diesel Material-to-Power Ratios (m^3/MW) for the Indicated Geothermal Technologies (postscript numbers indicate well depths [km]; error bars are ±1 standard deviation, representing well number variation for P/I , failed confirmation well variation for P/I/Ex; P_1 = 0.6)

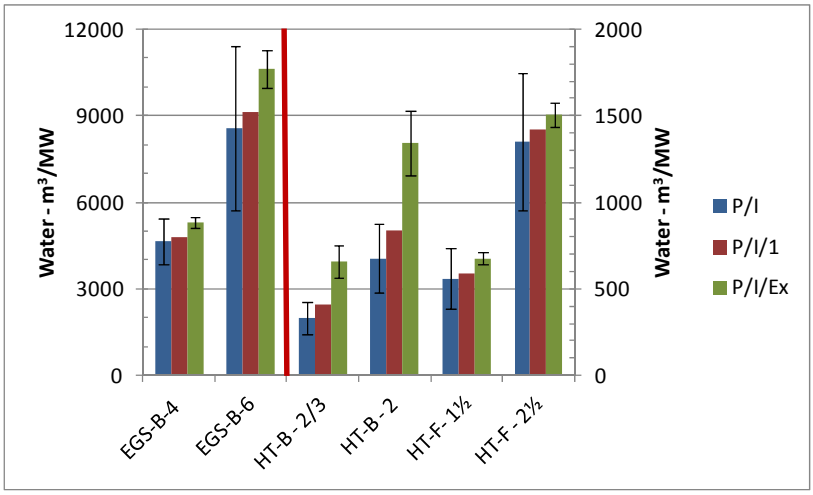

FIGURE A-5 Water Material-to-Power Ratios (m^3/MW) for the Indicated Geothermal Technologies (postscript numbers indicate well depths [km]; EGS values include 3,104 m^3/MW for injection well stimulation; EGS reads to the left and HT-B and HT-F read to the right; error bars are ±1 standard deviation, representing well number variation for P/I , failed confirmation well variation for P/I/Ex; P_1 = 0.6)

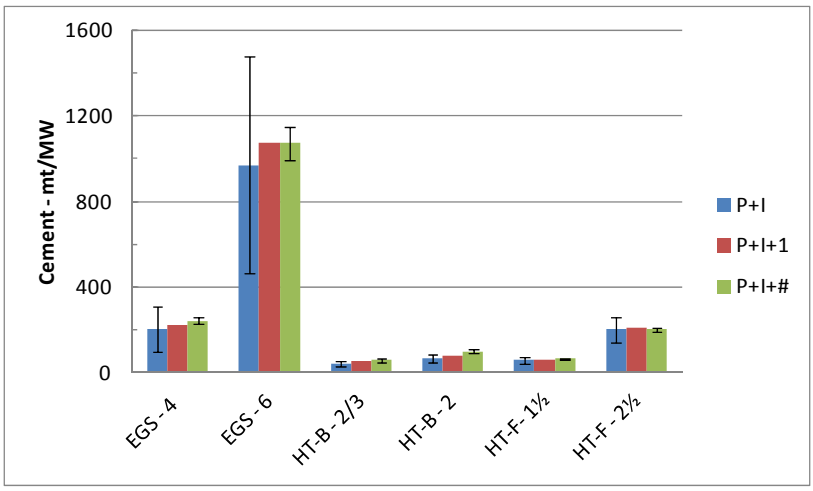

FIGURE A-6 Cement Material-to-Power Ratios (mt/MW) for the Indicated Geothermal Technologies (postscript numbers indicate well depths [km]; error bars are ±1 standard deviation, P+I set represent variation in well numbers, and P+I+# represent variation in confirmation well drilling; P_1 = 0.8)

TABLE A-5 Material-to-Power Ratios for Well Field Characterization[a]

Technology	Depth (km)	Capacity (MW)	N_p+N_I	Cement (mt/MW)			Steel (mt/MW)			Diesel[b] (m^3/MW)			Water[c] (m^3/MW)		
				P/I	P/I/1	P/I/Ex	P/I	P/I/1	P/I/Ex	P/I	P/I/1	P/I/Ex	P/I	P/I/1	P/I/Ex
EGS	4	20	9.6	203	224	289	304	336	431	124	135	237	4649	4810	5377
EGS	6	20	9.6	972	1073	1371	968	1069	1377	272	299	492	8565	9134	10.978
HT-B	2/3	10	4.2	42.6	52.6	81	50.8	62.6	100	20.1	24.8	59	334.5	412.3	669
HT-B	2	10	4.2	65.8	81.1	143	106.0	130.7	228	37.0	45.6	141	677.4	835.0	1504
HT-F	1.5	50	20.6	58	60	70	87	91	105	31	33	47	560	587	680
HT-F	2.5	50	20.6	200	210	221	236	247	261	45	47	71	1351	1417	1543

[a] N_P = number of P wells, N_I = number of I wells, P/I = production and injection wells only, P/I/1 = the same plus one additional production well, and P/I/E_x = P+I plus our model results for well field exploration. Cement and diesel columns are shaded so they can be read more easily.

[b] For EGS, 18.9 m^3/MW is included for stimulation of 3.2 injection wells.

[c] Values include EGS stimulation, which in this case is 3,104 m^3/MW for 3.2 injection wells at 19,400 m^3 per injection well.

TABLE A-6 2008 GHG Emissions, Electricity Generation, and Emission Rates for California Geothermal Power Production

Geothermal Power Plant	GHG Emissions (mt)[a]	Electricity Generated (MWh)[b]	GHG Emission Rate (g/kWh)	Running Capacity (MW)[c]
Bottle Rock	7,758	98,313	None reported	11
Cal Energy - J J Elmore	58,218	321,512	181.1	37
Cal Energy - J M Leathers	52,954	345,889	153.1	39
Cal Energy Region 1	203,886	1,300,030	156.8	153
Cal Energy Region 2	107,833	666,589	161.8	78
Geysers	194,896	6,020,595	32.4	725
Coso Finance Navy I	53,128	625,568	84.9	100
Coso Power Navy II	125,432	578,840	216.7	102
Coso Energy BLM E&W	121,742	489,670	248.6	100
Northern California Plant 1	5,584	490,544	11.4	52
Northern California Plant 2	8,470	456,196	18.6	56
Ormat GEM 2&3	28,692	184,861	155.2	21
Heber	4,687	324,099	14.5	38

[a] Data from California Environmental Protection Agency.
[b] Data from California Energy Commission.
[c] Data from Geothermal Energy Association.

TABLE A-7 2009 GHG Emissions, Electricity Generation, and Emission Rates for California Geothermal Power Production

Geothermal Power Plant	GHG Emissions (mt)[a]	Electricity Generated (MWh)[b]	GHG Emission Rate (g/kWh)	Running Capacity (MW)[c]
Bottle Rock	20,305	88,234	230.1	11
Cal Energy - J J Elmore	54,239	337,096	160.9	37
Cal Energy - J M Leathers	51,342	333,363	154.0	39
Cal Energy Region 1	223,562	1,324,696	168.8	153
Cal Energy Region 2	109,904	712,058	154.3	78
Geysers	172,522	5,949,433	29.0	725
Coso Finance Navy I	79,389	599,516	132.4	100
Coso Power Navy II	159,697	580,823	274.9	102
Coso Energy BLM E&W	184,767	510,566	361.9	100
Northern California Plant 1	6,033	471,128	12.8	52
Northern California Plant 2	7,159	431,927	16.6	56
Ormat GEM 2&3	28,414	184,806	153.8	21
Heber	4,116	367,818	11.2	38

[a] Data from California Environmental Protection Agency.
[b] Data from California Energy Commission.
[c] Data from Geothermal Energy Association.

TABLE A-8 2010 GHG Emissions, Electricity Generation, and Emission Rates for California Geothermal Power Production

Geothermal Power Plant	GHG Emissions (mt)[a]	Electricity Generated (MWh)[b]	GHG Emission Rate (g/kWh)	Running Capacity (MW)[c]
Bottle Rock	14,517	67,555	214.9	11
Cal Energy - J J Elmore	52,269	328,504	159.1	37
Cal Energy - J M Leathers	52,233	339,343	153.9	39
Cal Energy Region 1	216,737	1,241,259	174.6	153
Cal Energy Region 2	108,075	653,243	165.4	78
Geysers	159,873	5,981,055	26.7	725
Coso Finance Navy I	78,083	544,727	143.3	100
Coso Power Navy II	146,476	586,471	249.8	102
Coso Energy BLM E&W	173,442	459,285	377.6	100
Northern California Plant 1	5,549	454,623	12.2	52
Northern California Plant 2	7,277	391,184	18.6	56
Ormat GEM 2&3	22,637	242,606	93.3	21
Heber	3,813	None reported	None reported	38

[a] Data from California Environmental Protection Agency.
[b] Data from California Energy Commission.
[c] Data from Geothermal Energy Association.

TABLE A-9 2011 GHG Emissions, Electricity Generation, and Emission Rates for California Geothermal Power Production

Geothermal Power Plant	GHG Emissions (mt)[a]	Electricity Generated (MWh)[b]	GHG Emission Rate (g/kWh)	Running Capacity (MW)[c]
Bottle Rock	12,029	88,086	136.6	11
Cal Energy - J J Elmore	47,563	344,440	138.1	37
Cal Energy - J M Leathers	53,840	347,561	154.9	39
Cal Energy Region 1	178,376	1,246,941	143.1	153
Cal Energy Region 2	111,859	674,241	165.9	78
Geysers	222,631	5,973,368	37.3	725
Coso Finance Navy I	68,089	553,631	123.0	100
Coso Power Navy II	172,521	532,755	323.8	102
Coso Energy BLM E&W	178,408	406,742	438.6	100
Northern California Plant 1	23,648	435,683	54.3	52
Northern California Plant 2	29,397	422,781	69.5	56
Ormat GEM 2&3	24,987	199,540	125.2	21
Heber	None reported	292,042	None reported	38

[a] Data from California Environmental Protection Agency.
[b] Data from California Energy Commission.
[c] Data from Geothermal Energy Association.

TABLE A-10 2012 GHG Emissions, Electricity Generation, and Emission Rates for California Geothermal Power Production

Geothermal Power Plant	GHG Emissions (mt)[a]	Electricity Generated (MWh)[b]	GHG Emission Rate (g/kWh)	Running Capacity (MW)[c]
Bottle Rock	12,035	71,939	167.3	11
Cal Energy - J J Elmore	11,040	340,782	32.4	37
Cal Energy - J M Leathers	26,002	335,971	77.4	39
Cal Energy Region 1	68,346	1,092,351	62.6	153
Cal Energy Region 2	34,701	549,074	63.2	78
Geysers	224,571	6,114,921	36.7	725
Coso Finance Navy I	74,518	520,004	143.3	100
Coso Power Navy II	162,307	527,013	308.0	102
Coso Energy BLM E&W	178,107	358,848	496.3	100
Northern California Plant 1	23,145	458,243	50.5	52
Northern California Plant 2	27,020	416,600	64.9	56
Ormat GEM 2&3	23,751	189,782	125.1	21
Heber	None reported	None reported	None reported	38
Hudson Ranch Power I	None reported	352,755	None reported	50

[a] Data from California Environmental Protection Agency.
[b] Data from California Energy Commission.
[c] Data from Geothermal Energy Association.

TABLE A-11 Averages of and Ranges for Fuel Use Cycle GHG Emissions (g/kWh) from California HT-F Plants for the Years 2008, 2009, and 2010

Geothermal Power Plant	Average	+ Range	– Range
Bottle Rock	174.6	55.5	95.7
Cal Energy - J J Elmore	167.0	14.0	7.9
Cal Energy - J M Leathers	153.7	0.3	0.6
Cal Energy Region 1	166.7	7.9	9.9
Cal Energy Region 2	160.5	4.9	6.2
Geysers	29.4	3.0	2.6
Coso Finance Navy I	120.2	23.1	35.3
Coso Power Navy II	247.1	27.8	30.4
Coso Energy BLM E&W	329.4	48.3	80.8
Northern California Plant 1	12.1	0.7	0.7
Northern California Plant 2	17.9	0.7	1.3
Ormat GEM 2&3	134.1	21.1	40.8
Heber	12.8	1.6	1.6

This page intentionally blank.

Energy Systems Division
Argonne National Laboratory
9700 South Cass Avenue, Bldg. 362
Argonne, IL 60439-4815

www.anl.gov

Argonne National Laboratory is a U.S. Department of Energy
laboratory managed by UChicago Argonne, LLC